Chemical Engineering Science 326 (2026) 123437

Contents lists available at ScienceDirect

Chemical Engineering Science

journal homepage: www.elsevier.com/locate/ces

Optimal experimental design for guaranteed parameter estimation with rigorous formulation of the embedded liquid-liquid equilibrium

Daniel Jungen [a], Jan-Frederic Laub [a], Alexander Mitsos [b,a,c,*]

[a] Process Systems Engineering (AVT.SVT), RWTH Aachen University, Aachen, 52074, Germany
[b] JARA-CSD, Aachen, 52056, Germany
[c] Institute of Climate and Energy Systems: Energy Systems Engineering (ICE-1), Forschungszentrum Jülich GmbH, Jülich, 52425, Germany

ARTICLE INFO

Keywords:
Optimal experimental design
Bounded-error
Guaranteed parameter estimation
Liquid-liquid equilibrium
Baker's criterion

ABSTRACT

Semi-empirical models for liquid-liquid equilibrium (LLE) are essential for chemical process design but rely on experimental data for parameter estimation. In the face of high experimental costs, determining an informative experimental plan is crucial for constructing and validating these models efficiently. Optimal experimental design (OED) for (bounded-error) guaranteed parameter estimation (GPE) is a valuable approach to planning LLE experiments, but it has been limited to systems with simple input-output relations. We extend this method to systems whose input-output relation is implicitly given by an equation system with additional semi-infinite constraints, which corresponds to the rigorous computation of an LLE. Excess Gibbs free energy models are highly flexible but can predict spurious phase splits due to (i) using non-rigorous computations, or (ii) parameter values that are problematic in the sense that they lead to erroneous model behavior. To mitigate these issues in experiment planning, we (i) employ rigorous calculations using Baker's criterion, and (ii) enforce additional requirements, based on [Mitsos et al. Chem. Eng. Sci., 64(3):548-559, 2009] to exclude parameter values that lead to erroneous model behavior. We solve the resulting problem using (generalized) semi-infinite programming techniques and provide a proof of concept using the Redlich-Kister model to plan the OED to reduce parameter uncertainty. Our approach successfully avoids wrong predictions due to problematic parameter values and computes an experimental design that significantly reduces the predicted parameter uncertainty. However, our method is computationally demanding, necessitating advancements in numerical methods for practical applications involving multiple parameters or more complex excess models.

1. Introduction

Process simulations are an integral component of chemical engineering, playing a crucial role in tackling global challenges such access to clean water or responsible production. The semi-empirical models used therein, typically depend on semi-empirical thermodynamic models which inherently include mixture-dependent parameters that need to be estimated based on experiments (Kontogeorgis et al., 2021). Considering the limited availability of resources, including limited experimental resources, optimal experimental design (OED) is an indispensable approach that can help guide experimental efforts, maximizing knowledge gain while minimizing resource consumption and costs (Franceschini and Macchietto, 2008).

Model development for process simulations typically involves three key steps. Note that the following steps are usually not carried out in one single sequence but in an iterative manner (Franceschini and Macchietto, 2008). After some preliminary tests have been conducted, the model structure is defined (i), which usually relies on semi-empirical thermodynamic models, e.g., NRTL (Renon and Prausnitz, 1968), Redlich-Kister (Redlich and Kister, 1948), UNIQUAC (Abrams and Prausnitz, 1975), modified Wilson (Tsuboka and Katayama, 1975), or other excess models (Pfennig, 2004). Exceptions are predictive models; e.g.; (PC(P))-SAFT (Gross and Sadowski, 2001; Gross and Vrabec, 2006; Chapman et al., 1990), predictive PCP-SAFT (Nhu et al., 2008), COSMO-RS (Klamt, 1995) and data-driven predictive models using; e.g.; transformers (Winter et al., 2022), graph neural networks (Medina et al., 2022; Qin et al., 2023; Rittig et al., 2023; Medina et al., 2023), or matrix completion methods (Jirasek et al., 2022; Chen et al., 2021); which we do not consider in this work. (ii) Experiments are designed and conducted to collect measurement data. (iii) The measurement data are utilized for parameter estimation.

In step (i), model building, OED can be applied for model identification and discrimination (Box and Hill, 1967; Karimshoushtari and Novara, 2020). In step (ii), after the model structure has been

* Corresponding author.
E-mail addresses: daniel.jungen@avt.rwth-aachen.de (D. Jungen), jalaub@ethz.ch (J.-F. Laub), amitsos@alum.mit.edu (A. Mitsos).

https://doi.org/10.1016/j.ces.2026.123437
Received 10 July 2025; Received in revised form 16 January 2026; Accepted 22 January 2026
Available online 24 January 2026

identified, OED for parameter estimation can be used to increase parameter precision (Franceschini and Macchietto, 2008; Atkinson et al., 2007).

This contribution is only concerned with step (ii): specifically, we advance OED for guaranteed parameter estimation (GPE). Note that we assume no structural system-model mismatch and do not consider any problems arising from numerical difficulties. Our envisioned OED application is as follows. For many separation and purification processes, it is necessary to determine a liquid-liquid equilibrium (LLE) model. Often, initial measurement data of a temperature-dependent LLE miscibility gap is available and the model structure has been already defined. Using these data, a parameter estimation was conducted to obtain an initial guess for the parameter values of the underlying excess model utilized in modeling the LLE. In our contribution, our objective is to plan an optimal experiment in the GPE setting to further reduce the predicted parameter uncertainty in the underlying excess model. Note that if an inadequate model is being used, all efforts to reduce the predicted parameter uncertainty may be in vain. Therefore, the underlying excess model must be selected with great care, and it should be reassessed repeatedly to determine whether the chosen model is adequate. In existing OED approaches, usually only the necessary criterion for phase stability is used to predict the LLE because enforcing the sufficient condition leads to an embedded optimization problem, or equivalently to a semi-infinite constraint. This may lead to wrong predictions and subsequently to additional experimental effort. Further, wrong predictions may be obtained through *problematic* parameter values in the sense that incorrect phase splits or the prediction of more phases than observed are predicted. To avoid wrong predictions through the mentioned causes, we (i) extend OED for GPE for systems whose input-output relation is implicitly given by an equation system with additional semi-infinite constraints, which in our case is an LLE application and (ii) present an algorithmic adaption of existing algorithms for the solution of the resulting hierarchical optimization problem. In our formulation, we use the sufficient condition for phase stability and additionaly include constraints to avoid *problematic* parameter values. Last but not least, we present (iii) a proof-of-concept case study reducing the predicted parameter uncertainty.

1.1. Optimal experimental design for parameter estimation

OED for parameter estimation can be categorized into two main approaches: statistical OED (e.g., refer to Pronzato (2008), Aster and Thurber (2013) reviewing theory, and Franceschini and Macchietto (2008) reviewing applications) and bounded-error OED methods (Pronzato and Walter, 1990). Statistical OED methods are often based on maximum likelihood methods and aim to minimize the estimated parameter variances by considering the stochastic characteristic of the measurement uncertainties and their impact on the parameter uncertainty (Franceschini and Macchietto, 2008). These statistical methods are justifiable if the stochastic characteristics of measurement uncertainties are known, as is often the case (Dong et al., 2005). On the other hand, the necessary assumptions for the statistical methods are sometimes not met or challenging to verify (Milanese and Belforte, 1982; Dai et al., 2019) or repeated measurements are not feasible (Belforte et al., 1987; Marvel and Williams, 2012). In these cases, bounded-error OED methods can be applied because they do not rely on statistical assumptions and do not propose replicate experiments (Pronzato and Walter, 1989). Bounded-error OED methods assume that the measurement error is bounded and additive, with no other hypothesis concerning their statistical distribution (Pronzato and Walter, 1990; Walz et al., 2018).

More specifically, (bounded-error) OED for GPE computes an experimental design (to be carried out) that minimizes the estimated size of the feasible parameter set or an over-approximation thereof (Pronzato and Walter, 1990). The feasible parameter set[1] consists of all parameter values consistent with the model, the measurements, and their unknown but bounded measurement errors.

OED for GPE methods builds on the concepts of GPE, also known as set-membership or bounded-noise parameter estimation (Walter and Piet-Lahanier, 1990; Milanese and Vicino, 1991). A small size of the feasible parameter set corresponds to high parameter reliability. As computing the exact feasible parameter set, and therefore also the OED for GPE, is often time-consuming (Milanese and Belforte, 1982; Walz et al., 2018; Norton, 1987), ellipsoid, orthotropic (Milanese and Vicino, 1991; Belforte et al., 1990) or other approximations (Belforte and Tay, 1993; Belforte and Gay, 2000, 2004; Schweppe, 1968) are used instead.

For earlier works on OED for GPE, refer to Belforte et al., 1987; Pronzato and Walter, 1989; Norton, 1987; Belforte et al., 1984, who give an overview of linear models, and Pronzato and Walter, 1990; Belforte et al., 1988, for the nonlinear case. In more recent years, Borchers and co-worker(s) employ OED for GPE to discrete-time systems that are linear in the parameters and compute a one-step (Borchers et al., 2011) (multi-step (Borchers and Findeisen, 2011)) input design to minimize the volume of the feasible parameter set. Marvel and Williams, 2012 consider nonlinear continuous-time systems and leverage interval analysis to compute the next experiment design. Hasenauer et al. (2010) consider a class of implicit nonlinear discrete-time systems and apply their OED for GPE approach to a biochemical reaction network. Both, Marvel and Williams (2012), Hasenauer et al. (2010), compute discrete optimal inputs.

In a series of papers (Mukkula and Paulen, 2016a,b, 2017a), Gottu Mukkula and Paulen compute the OED for GPE for various applications by first overapproximating the feasible parameter set and then determining the next experiment to minimize the estimated overapproximation of the feasible parameter set. Through over-approximation of the feasible parameter set by a box, the OED for GPE problem becomes a min-max bilevel program (BLP). This BLP is, up to this point, a rigorous and general method of OED for GPE. Gottu Mukkula and Paulen solve this BLP by replacing the lower-level problem (LLP) with its KKT conditions, which leads to a mathematical program with equilibrium constraints. They note that one must ensure that the solution of the mathematical program with equilibrium constraints is globally optimal in the LLP (Mukkula and Paulen, 2016a). Their earlier works (Mukkula and Paulen, 2016a,b) do not guarantee global optimality in the LLP, but they later propose an *a posteriori* check for verifying global optimality in the LLP (Mukkula and Paulen, 2016b) and a heuristic for cases where this check fails (Mukkula and Paulen, 2017a). Mukkula and Paulen (2017a) note that their heuristic leads to an increased probability of identifying local optima of the OED problem.

In Walz et al. (2018), we build on the work of Mukkula and Paulen (2017a) by applying a solution method that guarantees a global solution to the OED problem. We employ an algorithm based on our prior work (Mitsos and Tsoukalas, 2015) for generalized semi-infinite programs (GSIPs), which is simplified to the min-max bilevel structure of the OED problem. First-order necessary conditions of the LLP are not used therein. Note that the usage of semi-infinite programming techniques is not novel (Žaković and Rustem, 2003; Rustem and Howe, 2002). In Walz et al. (2018), we were able to obtain a global solution for the simple case study, but not for the more complex case studies. The bottleneck is whether the used subsolver converges in a reasonable time.

In the OED formulation of previous works (Walz et al., 2018; Mukkula and Paulen, 2016a,b, 2017a) an explicit analytical input-output relation is required for the underlying model. This restriction might be one of the reasons why OED for GPE is still considered infeasible in flow sheeting software (Asprion et al., 2020). This also motivates this work, where we extend OED for GPE for systems whose input-output

[1] The feasible parameter set is also called feasible parameter region (Norton, 1987), parameter uncertainty set (Belforte et al., 1988), set of consistent parameters (Hasenauer et al., 2010), consistent parameter set (Borchers et al., 2011), or (model) membership set (Pronzato and Walter, 1989).

relation is implicitly given by an equation system with additional semi-infinite constraints.

In contrast to classical approaches, such as Fisher information-based approaches, bounded-error OED methods perform a worst-case experimental design, which safeguards against experiments that perform well on average but poorly for certain parameter values. In bounded-error OED, minimizing the volume of the feasible parameter set (which corresponds to the 100 % non-asymptotic confidence region (Pronzato and Walter, 1989)), also called V-optimal design, can be seen as the natural counterpart to classical/statistical D-optimal design, where the joint confidence ellipsoids are minimized (Theorem 1 in Pronzato and Walter, 1990). Marvel and Williams, 2012 provide a comparision of their bounded-error OED approach to traditional V- and D-optimality design criteria.

For other closely connected OED approaches, the interested reader may refer to Asprey and Macchietto, 2002; Welsh and Rojas, 2009; Mukkula et al., 2021; Mukkula and Paulen, 2022; Denis-Vidal et al., 2019; Mukkula and Paulen, 2017b; Walz et al., 2020.

1.2. Notions on generalized and semi-infinite programming

In OED, we encounter concepts and notions of bilevel and (generalized) semi-infinite programming because the definition of the objective and/or constraints of the OED problem involves solving a lower-level optimization problem. BLPs and (generalized) semi-infinite programs ((G)SIP) consist of two levels, an upper level and a lower level. Note that one must solve the LLP to global optimality to check the feasibility of a given candidate solution point. The BLP or GSIP can be reformulated as a single-level problem if the LLP satisfies regularity conditions and is convex (Dempe, 2002). However, in our OED application, the LLP is inherently nonconvex because the nonconvexity of the Gibbs free energy function is necessary to model a phase split. In recent years, several methods have been proposed for hierarchical problems that do not rely on convexity assumptions. For more details, the interested reader may refer to our recent literature review (Djelassi et al., 2021).

In our contribution, we apply an adaptive discretization-based approach, which builds on the approach of Blankenship and Falk (1976) and its successors. Blankenship and Falk (1976) present an algorithm for solving SIPs, i.e., an optimization problem that is constrained by a parametric constraint. This parametric constraint is defined through an index set of infinite cardinality. For a general formulation of an SIP, refer to (B.1) in Appendix B. Blankenship and Falk (1976) replace the infinite index set by a finite discretized set. This discretized problem is an approximation of the original SIP, more precisely, a relaxation. The approximation of (B.1) is iteratively improved through an adaptive refinement scheme. Conceptually, the successors Mitsos and Tsoukalas (2015), Djelassi et al. (2019), Falk and Hoffman (1977), which we will use to solve the OED problem in this contribution, apply the same adaptive discretization-based procedure as Blankenship and Falk (1976). Note that these successors (Mitsos and Tsoukalas, 2015; Djelassi et al., 2019) utilize an upper-bounding procedure to find a global solution that is SIP-feasible, c.f., Definition 2 in Appendix B. However, in our application, the necessary assumption for the upper-bounding procedures is not satisfied. As a result, we rely solely on the relaxation-based lower-bounding procedure.

1.3. Modeling liquid-liquid equilibria

Two main approaches exist for modeling LLEs. The first approach relies on solving nonlinear equations, which correspond to the first derivatives of the Gibbs free energy, i.e., equal activities, and the mass balances. The second approach directly minimizes the Gibbs free energy or solves a related optimization problem.

Methods of the first approach rely on the isopotential condition, which uses the property that a system is in equilibrium if the thermodynamic potential is equal across all phases. Many numerical methods have been developed to solve these challenging nonlinear equations; however, a fundamental problem is that thermodynamically incorrect solutions are often predicted, such as erroneous phases or trivial solutions that mistakenly suggest a homogeneous mixture. This is because the first approach relies on the isopotential condition to compute stationary points, i.e., local minima, maxima, or saddle points of the Gibbs free energy curve. The isopotential condition is only a necessary condition for phase stability, and the predicted solutions can be unstable (Sørensen et al., 1979). However, these methods are used more frequently (often, with appropriate *good* initial guesses to avoid trivial solutions) because the second approach, while being more reliable in practice, is computationally more demanding.

Methods of the second approach can be broadly categorized into three categories (Marcilla et al., 2010): (i) Michelsen (1982a,b) present a stability condition, which can be geometrically interpreted as the vertical distance between the tangent hyperplane and the Gibbs free energy surface, and use this condition in their phase split calculations. The presented stability condition of Michelsen (1982a,b) is closely connected to the tangent plane (TP) criterion of Baker et al. (1982), also called Gibbs TP. We propose in Mitsos and Barton (2007) a stability condition based on the Lagrangian dual of the Gibbs TP stability criterion. The solution of the dual problem describes the stable phase split. Notably, our method permits very weak assumptions: An unknown, even infinite, number of phases is allowed; it is not required that all species are present in every phase; and the Gibbs free energy must only be continuous. (ii) Eubank et al. (1992) present the area method, where they maximize the integrated area between the TP and the Gibbs surface. (iii) Eubank and Hall (1995) present an equal area rule which uses a similar concept to the *van der Waals* loop. The equal area rule and modifications thereof, e.g., Sapkowski and Hofman (2023), find the common tangent line, which corresponds to finding an equal area construction for the derivative of the total Gibbs free energy.

Partially due to the inherent flexibility of the excess model, LLEs have been successfully predicted with both approaches. While this flexibility is advantageous in some cases, it can also be problematic. Parameter values can be *problematic* in the sense that incorrect phase splits or the prediction of more phases than observed are predicted (Mitsos et al., 2009a; Bollas et al., 2009). These issues can arise regardless of the approach used to compute the LLE. Marcilla et al. (2017) show that an unexpectedly high number of (randomly selected) publications include *problematic* parameter values and predicted LLE data that are inconsistent, i.e., predictions do not agree with experimental data, tie-lines do not satisfy Gibbs stability criteria, or even the isopotential condition is not satisfied. Eight years later, Marcilla et al. (2025) show that these challenges remain.

In this work, we use ideas from our previous work (Mitsos et al., 2009a), which resolves the limitations of standard parameter estimation methods that may produce *problematic* parameter values. Mitsos et al. (2009a) use the Gibbs TP criterion to check stability *during* parameter estimation and, additionally, introduces a series of conditions to exclude *problematic* parameter values. The conditions for excluding *problematic* parameter values essentially constrain the curvature of the Gibbs surface through local convexity conditions and confining the Gibbs surface between tangent and secant lines. The Gibbs TP criterion and the additional conditions to exclude *problematic* parameter values are written as (generalized) semi-infinite constraints and ensure that only the observed phase behavior is predicted with the obtained parameter values.

In a somewhat related fashion to Mitsos et al. (2009a), Marcilla et al. (2010) present a software that uses a robust computation algorithm to fit parameter values of excess models to equilibria data. Their method is robust in the sense that they exclude *problematic* parameter values. The method employs some topology analysis of the Gibbs energy of mixing. They enforce, as in our work (Mitsos et al., 2009a), local convexity conditions and also some empirically derived restrictions. In contrast to Mitsos et al. (2009a), they do not write their conditions as (generalized) semi-infinite constraints, but enforce them on a grid of points. They suc-

cessfully apply their method to multiple multi-component systems (e.g., Olaya et al., 2008; Reyes-Labarta et al., 2009; Gomis, 2011).

1.4. Optimal experimental design for liquid-liquid equilibria characterization

If the semi-empirical model used in process simulations is not predictive, its parameters must be fitted to experimental data. However, the thermodynamic functions, e.g., the activity, can not be measured directly. LLE data can be used to estimate parameters included in excess models, as the chemical potentials of the components are equal at equilibrium. A standard method for characterizing an LLE involves adding the components to a closed vessel in known quantities, stirring, and tempering the vessel until equilibrium is reached. After equilibration, samples are taken from both phases, and their compositions are subsequently determined. Finally, the parameters of the excess model are fitted to the LLE data (Pfennig, 2004).

OED possesses great potential for characterizing LLEs because conducting LLE measurements is cost- and labor-intensive. OED enables efficient planning that minimizes laboratory effort while still reducing parameter uncertainty. Usually, Fisher information-based criteria are used for OED and the LLE is modeled using the isopotential condition (Dechambre et al., 2014; Duarte et al., 2019). However, due to the high cost of experiments, measurement data may be scarce, which raises the question of whether the necessary assumptions for the classical/statistical methods, i.e., assumptions concerning the stochastic characteristics of the measurement uncertainties, are satisfied. Additionally, the planned experimental designs may be suboptimal in the sense that the planned experiment does not provide informative measurement data, leading to additional experimental effort. For example, the experimental design could suggest compositions to the experimenter where the available data does not indicate any phase splitting. This may be caused by wrong LLE predictions resulting from, e.g., modeling the LLE solely with the isopotential condition or using *problematic* parameter values for the local composition models. As the utmost goal should be to minimize experimental effort, we propose to use an OED for GPE approach for planning the next experiment design, (i) base our computations of the LLE predictions on the sufficient condition for phase stability, i.e., the Baker's criterion (Baker et al., 1982), and (ii) impose the additional conditions of Mitsos et al. (2009a) onto the parameter values such that erroneous predictions due to *problematic* parameter values are avoided and the feasible parameter set is more tightly approximated by excluding *problematic* parameter values. Our proposed formulation leads to a generalized min-max problem with embedded (generalized) semi-infinite constraints. We solve this problem using a specialization of the generalized semi-infinite algorithm, based on Mitsos and Tsoukalas (2015), Djelassi et al. (2019), Falk and Hoffman (1977).

The contribution is organized as follows. In Section 2.1, we recapitulate the thermodynamic background for modeling LLEs and the ideas of Mitsos et al. (2009a) to exclude *problematic* parameter values that may lead to wrong predictions. Section 2.2 covers OED for GPE and its application to the intended LLE application. Furthermore, we present a specialized algorithm for solving the introduced OED for GPE problem and the necessary subproblems used in the solution procedure. Section 3 presents an illustrative case study, using the Redlich-Kister model as the excess model. In Section 4, we review the current limitations of our propsed method and provide an outlook and potential directions for future research. We conclude our work in Section 5.

2. Methodology

In the following section, we present the methodology for addressing our three contributions, namely (i) extending OED for GPE for systems whose input-output relation is implicitly given by an equation system with additional semi-infinite constraints, which in our case is an LLE application, (ii) presenting an algorithmic adaption for the solution of the resulting hierarchical optimization problem, and (iii) plan an OED for a proof-of-concept application.

2.1. Thermodynamic background

In the following, we provide a short review of the thermodynamic background necessary for modeling LLEs and concepts presented by Mitsos et al. (2009a) to exclude *problematic* parameter values that could result in inaccurate predictions. We consider a binary two-phase system, as local composition models such as NRTL (Renon and Prausnitz, 1968) are based exclusively on binary interaction parameters. Three- and higher multi-component systems are described with permutations of the binary interaction parameters between all species. Hence, LLE data of binary systems is already sufficient, avoiding the need for very costly multi-species experiments. Note that an extension to multicomponent systems is, in principle, straightforward, but would drastically increase the computational effort.

For simplification purposes, we assume non-vanishing phases and that all species are present in all phases. As is typically the case in LLE computations, we neglect the pressure influence (Stephan et al., 2017). We would like to emphasize that our simplifications may be restrictive, particularly near the critical point, when phases disappear, or in cases of structural system-model mismatch. Because we do not consider reactions, the total number of moles (of each species) is constant, and we can omit the molar Gibbs free energy of formation (Pfennig, 2004). Therefore, we can base our computations using the mole fractions and molar quantities of the Gibbs free energy of mixing $\bar{G}^{\mathrm{M}}$. Using the closing condition and mass balances, we can eliminate all describing state variables except for the mole fraction of the first species in the first phase, x_1, and the mole fraction of the first species in the second phase, x_2. For notational convenience, we arbitrarily enforce without loss of generality that $x_1 \leq x_2$. The derivative of the molar Gibbs free energy of mixing $\frac{\partial \bar{G}^{\mathrm{M}}}{\partial x}\Big|_{\bar{T},\bar{\boldsymbol{p}},x}$ is indefinite at $x = 0$ and $x = 1$ and approaches $-\infty$. As infinity is difficult to handle for optimization solvers, we restrict the mole fractions to $x \in \left[x_{\min}, 1 - x_{\min}\right] := \mathcal{X}$, with $x_{\min} > 0$. However, for small $x_{\min}$ this is not restrictive, as we assume that each species is present in each phase (Mitsos et al., 2009a). For ease of notation, we define $x_{\mathrm{L}} = x_{\min}$ and $x_{\mathrm{U}} = 1 - x_{\min}$ and aggregate the mole fractions of the phases in the vector $\boldsymbol{x} = \left(x_1, x_2\right)^T$.

2.1.1. Modeling liquid-liquid equilbria

In the following, we reiterate the isopotential condition and TP criterion by Baker et al. (1982), which we use to model the LLE. We will highlight how the TP criterion results in a semi-infinite constraint. The isopotential condition reads for a (binary) two-phase system described by $\bar{\boldsymbol{x}}$ at constant temperature $\bar{T}$

$$\begin{aligned} \gamma_1\left(\bar{T},\bar{\boldsymbol{p}},\bar{x}_1\right)\cdot\bar{x}_1 &= \gamma_1\left(\bar{T},\bar{\boldsymbol{p}},\bar{x}_2\right)\cdot\bar{x}_2 \\ \gamma_2\left(\bar{T},\bar{\boldsymbol{p}},\bar{x}_1\right)\cdot\left(1-\bar{x}_1\right) &= \gamma_2\left(\bar{T},\bar{\boldsymbol{p}},\bar{x}_2\right)\cdot\left(1-\bar{x}_2\right), \end{aligned} \tag{1}$$

with γ_i being the activity coefficient of component i, and $\bar{\boldsymbol{p}}$ being the parameters of the underlying excess model (Pfennig, 2004). Recall that (1) together with the mass balances (simplifications see Appendix A.1), is only a necessary condition for phase stability, which, if solely used, may lead to wrong predictions. Incorrect predictions may lead to additional experimental effort. To minimize experimental effort in the laboratory, we also enforce the TP criterion.

The TP criterion reads (Baker et al., 1982)

$$\bar{G}^{\mathrm{M}}\left(\bar{T},\bar{\boldsymbol{p}},\bar{x}_1\right) + \frac{\partial \bar{G}^{\mathrm{M}}}{\partial x}\Big|_{\bar{T},\bar{\boldsymbol{p}},\bar{x}_1}\left(y-\bar{x}_1\right) \leq \bar{G}^{\mathrm{M}}\left(\bar{T},\bar{\boldsymbol{p}},y\right),\ \forall y \in \mathcal{X}. \tag{2}$$

The dummy symbol y is introduced instead of x to emphasize the key differences between them: y is the worst-case realization from the set $\mathcal{X}$ in (2), while x corresponds to the model output. (2) is a semi-infinite constraint and can not be implemented in or handled by standard (MI)NLP solvers. Therefore, in adaptive-discretization based methods for SIPs,

Table 1
Tabular overview of the conditions in the OED problem. For a graphical interpretation see Fig. 1.

Equation	Description	Implications for LLE predictions	Constr. type	Discretized condition	Corresp. subproblem
(1)	Isopotential condition	with mass balances necessary condition for phase stability	Equality	–	–
(2)	TP critereon	with mass balances sufficient condition for phase stability	SIP	(3)	(4)
(5)	$\bar{G}^{\mathrm{M}}$ locally convex at x_1 and x_2	implied by (2); enforced for computational speed up	Equality	–	–
(6)	$\bar{G}^{\mathrm{M}}$ convex outside the phase split	no erroneous phase splits predicted outside the observed phase split	GSIP	(7) & (8)	(9) & (10)
(11) & (12)	TP constructed near $x \approx 0$ & $x \approx 1$ below $\bar{G}^{\mathrm{M}}$	no erroneous phase splits predicted outside the observed phase split	SIP	(13) & (14)	(15) & (16)
(17)	Secant strictly below $\bar{G}^{\mathrm{M}}$ in the interior of the phase split	no metastable phase splits predicted inside the observed phase split	GSIP	(18)	(19)

the constraint is discretized and relaxed to

$$\bar{G}^{\mathrm{M}}(\bar{T},\bar{\boldsymbol{p}},\bar{x}_1) + \left.\frac{\partial \bar{G}^{\mathrm{M}}}{\partial x}\right|_{\bar{T},\bar{\boldsymbol{p}},\bar{x}_1} (y^d - \bar{x}_1) \leq \bar{G}^{\mathrm{M}}(\bar{T},\bar{\boldsymbol{p}},y^d), \tag{3}$$

with $y^d \in \mathcal{X}^{\mathrm{DISC}} \subsetneq \mathcal{X}$. In the implementation, we approximate the derivative $\left.\frac{\partial \bar{G}^{\mathrm{M}}}{\partial x}\right|_{\bar{T},\bar{\boldsymbol{p}},\bar{x}_1}$ with $\frac{\bar{G}^{\mathrm{M}}(\bar{T},\bar{\boldsymbol{p}},\bar{x}_2)-\bar{G}^{\mathrm{M}}(\bar{T},\bar{\boldsymbol{p}},\bar{x}_1)}{\bar{x}_2-\bar{x}_1}$ because preliminary investigations have shown that this formulation slightly reduces the computation burden for binary systems.

The solution procedure employed in this contribution uses the relaxed TP criterion (3) in conjunction with (1), and mass balances. The predicted phase split $\bar{\boldsymbol{x}}$ (for given $\bar{T}$ and $\bar{\boldsymbol{p}}$) is stable, if the optimal objective value of

$$f^{(4)} = \max_{y \in \mathcal{X}} \quad \bar{G}^{\mathrm{M}}(\bar{T},\bar{\boldsymbol{p}},\bar{x}_1) + \left.\frac{\partial \bar{G}^{\mathrm{M}}}{\partial x}\right|_{\bar{T},\bar{\boldsymbol{p}},\bar{x}_1} (y - \bar{x}_1) - \bar{G}^{\mathrm{M}}(\bar{T},\bar{\boldsymbol{p}},y), \tag{4}$$

is equal to 0. Note that in (4) and all following equations the symbols have superscript and subscript numbers in parentheses to indicate their association with the corresponding equation. Standard NLP solvers can only solve an NLP to a certain tolerance. Therefore, we consider $\bar{\boldsymbol{x}}$ feasible, i.e., it describes the LLE, if the optimal objective value of (4) is less equal to a small $\varepsilon^{\mathrm{a},(4)} > 0$. If $f^{(4)} > \varepsilon^{\mathrm{a},(4)}$, the predicted phase split is not stable and the solution of (4) is used to refine the discretization $\mathcal{X}^{\mathrm{DISC}}$ and the LLE computations are repeated.

In our experience, additionally adding the constraint that $\bar{G}^{\mathrm{M}}$ is locally convex at x_1 and x_2 accelerates convergence (Mitsos et al., 2009a). This constraint, which is implied by (2), reads

$$\left.\frac{\partial^2 \bar{G}^{\mathrm{M}}}{\partial x^2}\right|_{T,\boldsymbol{p},x_i} \geq 0, \ \forall i, \tag{5}$$

where x_i denotes the composition of the two phases. Hence, in the implementation, (5) is added as a constraint.

The excess Gibbs free energy included in $\bar{G}^{\mathrm{M}}$, c.f., Appendix A.2, is typically computed using NRTL (Renon and Prausnitz, 1968), Redlich-Kister (Redlich and Kister, 1948), UNIQUAC model (Abrams and Prausnitz, 1975), modified Wilson model (Tsuboka and Katayama, 1975), or other excess models (Pfennig, 2004). Pragmatically, the Redlich-Kister model, c.f., (A.3) in Appendix A.2, is chosen in this contribution as a proof-of-concept. This relatively simple excess model is chosen to reduce the computational burden. Note that the proposed OED for GPE method is in theory directly applicable to other excess models; however, it would result in higher computational demand. Further note that the computational burden is the bottleneck of the proposed OED method, c.f., Section 3, and using more complex excess models is currently not computationally feasible.

2.1.2. Conditions for the exclusion of problematic parameter values

While local composition models have been successfully used to predict LLEs, their flexibility has been proven to lead to wrong predictions (predicting wrong phase splits or more phases than measured, modeling homogeneous azeotropes as heterogeneous, etc. (Mitsos et al., 2009a; Bollas et al., 2009; Marcilla et al., 2017, 2025)). For example, consider a binary mixture that has one observed liquid-liquid split at x_1 and x_2 for a total composition x_{total}. Fig. 1a shows the Gibbs free energy of mixing $\bar{G}^{\mathrm{M}}$ used to model this LLE. If the total composition is between $x_1 < x_{\mathrm{total}} < x_2$ and a rigorous method is used for the predictions, the observed phase split is predicted. However, if the total composition is, e.g., x'_{total}, the spurious phase split at $\approx x'_1$ and $\approx x_1$ is predicted; even if a rigorous method is being used. This is due to $\bar{G}^{\mathrm{M}}$ being non-convex on the left-hand side of x_1. Therefore, the corresponding parameter values are considered *problematic*. This example also highlights the drawbacks if only the necessary isopotential condition (1) is used for the predictions without (2). Then, for x_{total} the phase split with the common tangent line at x'_1 and $\approx x_2$ may be wrongly predicted. Note that the wrong phase split prediction between x'_1 and $\approx x_2$ fulfill condition (1) but not (2). To exclude such *problematic* parameter values, the model predictions are usually checked *after* parameter estimation. Otherwise, as in our example, incorrect predictions may be encountered in the modeled processes if these *problematic* parameters are used. The method proposed by Mitsos et al. (2009a) addresses the limitations of standard parameter estimation methods. Mitsos et al. (2009a) introduce a series of conditions to check stability *during* parameter estimation to exclude these *problematic* parameter values. The inclusion of these conditions into the parameter estimation leads to a BLP.

We have utilized and extended rigorous parameter estimation, excluding *problematic* parameter values, in several extensions (Bollas et al., 2009; Mitsos et al., 2009b; Glass et al., 2017, 2018; Glass and Mitsos, 2017, 2019), considering a variety of thermodynamic systems. Note that the methods have been implemented in the software package Bilevel Optimization Algorithm for Rigorous & Robust Parameter Estimation in Thermodynamics (BOARPET) (Mitsos et al., 2018) and that BOARPET is also available as a plugin to the DECHEMA package DPP (DECHEMA e.V., 2024).

In this contribution, we utilize the idea of Mitsos et al. (2009a) of checking phase stability during parameter estimation by including it directly into the OED for GPE. In contrast to Mitsos et al. (2009a), who require that their additional conditions for parameter values $\bar{\boldsymbol{p}}$ *only* hold for the measured temperatures, we require the conditions to hold for *all* possible temperature values, i.e., over a continuous temperature range. By pursuing our idea in Mitsos et al. (2009a) with greater rigor, the corresponding (generalized) semi-infinite constraints become multidimensional and, as such, more difficult. If the conditions outlined by Mitsos et al. (2009a) are satisfied over the entire temperature range for a given set of parameter values, we postulate that the resulting LLE predictions are unique, e.g., no additional (wrong) phases are predicted. By including phase stability checks into the OED framework, we aim to ensure that (i) the planned experiments are meaningful — this may not be the case if a wrong phase split is predicted — and (ii) the prediction of $\boldsymbol{x}$ is unique. The second part is already included in the first, but it should be

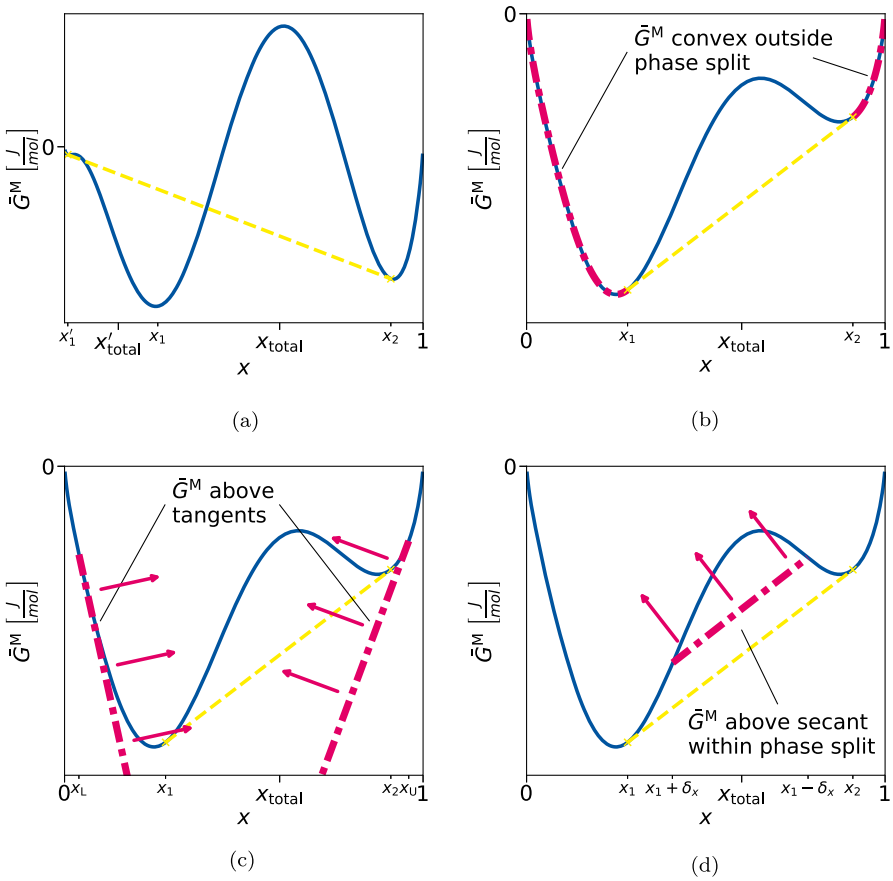

Fig. 1. Fig. 1a visualizes $\bar{G}^{\mathrm{M}}$ for parameter values which are not considered feasible. Fig. 1b to d visualize the conditions for parameter values $\bar{p}$ to be considered feasible by Mitsos et al. (2009a). Note that the visualization shows the respective conditions for a fixed temperature and not, as required in this contribution, over the whole temperature range $\mathcal{T}$. The phase split is denoted by x_1 and x_2. Yellow dashed lines represent the common tangent lines.
(a) Visualization of $\bar{G}^{\mathrm{M}}$ of parameter values $\boldsymbol{p}$, which may lead to wrong predictions (due to $\bar{G}^{\mathrm{M}}$ being non-convex left of x_1), making them *problematic*, and, thus, considered infeasible. Note that the shown common tangent line fulfills (1) but not (2). This tangent is only found if a non-rigorous solution method is used.
(b) Visualization of (6). To avoid erroneous predictions, $\bar{G}^{\mathrm{M}}$ should be convex with respect to the mole fraction outside the phase split. Parameter values, as used in 1(a), are excluded by the shown condition.
(c) Visualization of (11) and (12). The centers of the tangent expansion are x_{L} and x_{U}, respectively. To avoid erroneous predictions, $\bar{G}^{\mathrm{M}}$ should lie above the tangents. Parameter values, as used in 1(a), are excluded by the shown conditions.
(d) Visualization of (17). To avoid erroneous predictions, $\bar{G}^{\mathrm{M}}$ should lie above the shown secant in the interior of the phase split. Note that parameter values, as used in 1(a), are not excluded by the shown condition because the respective secant in the interior of the phase split x_1 and x_2 fulfills the shown condition.

emphasized as it is required by the solution algorithm, which is heavily based on Djelassi et al. (2019) (and specialized with ideas from Mitsos and Tsoukalas, 2015; Falk and Hoffman, 1977).

Mitsos et al. (2009a) consider a binary mixture with one liquid-liquid split over the temperature (and pressure) range under consideration. Mitsos et al. (2009a) motivate that parameter values $\bar{p}$ should only be considered feasible if $\bar{G}^{\mathrm{M}}$ is convex in x outside the phase split, the Gibbs TPs developed at x_{L} and x_{U} lies below the Gibbs free energy surface, and the secant, which is constructed approximately at the phase split, is strictly below the Gibbs surface within the phase split, c.f., Fig. 1b to d and Table 1.

Convexity of $\bar{G}^{\mathrm{M}}$ outside the phase split

The extended condition that $\bar{G}^{\mathrm{M}}$ must be convex on the whole temperature range with respect to the mole fraction outside the phase split, c.f. Fig. 1b, reads

$$\left.\frac{\partial^2 \bar{G}^{\mathrm{M}}}{\partial x^2}\right|_{T,\bar{p},y} \geq 0,\ \forall T \in \mathcal{T},\ \forall y \in [x_{\mathrm{L}}, x_1] \cup [x_2, x_{\mathrm{U}}]. \tag{6}$$

Note that x_1 and x_2 describe the phase split, depend on the (in the case of Mitsos et al. (2009a), measured) temperature T and parameter values $\bar{p}$, and must satisfy (2). (6) is a generalized semi-infinite constraint. Reformulation, relaxation, and discretization (akin (3)) of (6) yield two semi-infinite constraints (for the left- and right-hand side outside the phase split)

$$\min\left\{-\left.\frac{\partial^2 \bar{G}^{\mathrm{M}}}{\partial x^2}\right|_{T^d,\bar{p},y^d}, -\left(x_2^d - y^d\right)\right\} \leq 0 \tag{7}$$

and

$$\min\left\{-\left.\frac{\partial^2 \bar{G}^{\mathrm{M}}}{\partial x^2}\right|_{T^d,\bar{p},y^d}, -\left(y^d - x_1^d\right)\right\} \leq 0. \tag{8}$$

Note that $\boldsymbol{x}^d$ is implicitly defined through T^d, $\bar{p}$, (2), and mass balances. For fixed parameter values $\bar{p}$, we can check if these parameter values fulfill (7) and (8) for all possible values of $y \in \mathcal{X}$ by solving the subproblems

$$\begin{aligned} f^{(9)} = \max_{\substack{T\in\mathcal{T}, y\in\mathcal{X},\\ \boldsymbol{x}\in\mathcal{X}^2}} \quad & -\left.\frac{\partial^2 \bar{G}^{\mathrm{M}}}{\partial x^2}\right|_{T,\bar{p},y} \\ \text{s.t.} \quad & y \leq x_1 \\ & \text{(2) holds for } T, \bar{p}, \boldsymbol{x} \\ & \text{mass balances hold for } \boldsymbol{x} \end{aligned} \tag{9}$$

and

$$f^{(10)} = \max_{\substack{T\in\mathcal{T},y\in\mathcal{X},\\ \boldsymbol{x}\in\mathcal{X}^2}} \quad -\frac{\partial^2\bar{G}^{\mathrm{M}}}{\partial x^2}\Big|_{T,\bar{\boldsymbol{p}},y} \quad \text{s.t.} \quad x_2 \le y \quad (2) \text{ holds for } T,\bar{\boldsymbol{p}},\boldsymbol{x} \quad \text{mass balances hold for } \boldsymbol{x}. \tag{10}$$

Note that (9) and (10) are themselves SIPs with (4) being their corresponding LLPs, which can be solved with Algorithm 3 in Appendix B. If (the final lower bound of) the optimal objective value $f^{(9)}$ (and $f^{(10)}$) is less equal to $\varepsilon^{\mathrm{a},(10)}$, $\bar{\boldsymbol{p}}$ fulfills the corresponding condition. If not, the optimal solution T^* and y^* of (9) (and (10)) are used to discretize (7) (and (8)).

Note that the algorithm by Mitsos (2011) is not applicable for (9), (10), and (19) (to be introduced) because it requires an ε^{f}-optimal SIP-Slater Point, c.f. Definition 4 in Appendix B. However, an ε^{f}-optimal SIP-Slater Point does not exist in the considered cases because of (2).

Gibbs tangent plane below $\bar{G}^{\mathrm{M}}$ at the boundaries

The Gibbs TPs constructed near $x_{\mathrm{L}} \approx 0$ and $x_{\mathrm{U}} \approx 1$ must lie below $\bar{G}^{\mathrm{M}}$, c.f. Fig. 1c. This condition extended on $\mathcal{T}$ reads

$$\bar{G}^{\mathrm{M}}(T,\bar{\boldsymbol{p}},x_{\mathrm{L}}) + \frac{\partial\bar{G}^{\mathrm{M}}}{\partial x}\Big|_{T,\bar{\boldsymbol{p}},x_{\mathrm{L}}} (y - x_{\mathrm{L}}) \le \bar{G}^{\mathrm{M}}(T,\bar{\boldsymbol{p}},y),\ \forall T\in\mathcal{T},\ \forall y\in[x_{\mathrm{L}},x_{\mathrm{U}}] \tag{11}$$

and

$$\bar{G}^{\mathrm{M}}(T,\boldsymbol{p},x_{\mathrm{U}}) + \frac{\partial\bar{G}^{\mathrm{M}}}{\partial x}\Big|_{T,\bar{\boldsymbol{p}},x_{\mathrm{U}}} (y - x_{\mathrm{U}}) \le \bar{G}^{\mathrm{M}}(T,\bar{\boldsymbol{p}},y),\ \forall T\in\mathcal{T},\ \forall y\in[x_{\mathrm{L}},x_{\mathrm{U}}]. \tag{12}$$

These two conditions exclude parameter values that will predict additional spurious phase splits outside the true one (case E in Mitsos et al., 2009a), e.g., parameter values producing a $\bar{G}^{\mathrm{M}}$ curve as depicted in Fig. 1a would be excluded. Again, discretizing using index d yields

$$\bar{G}^{\mathrm{M}}(T^d,\bar{\boldsymbol{p}},x_{\mathrm{L}}) + \frac{\partial\bar{G}^{\mathrm{M}}}{\partial x}\Big|_{T^d,\bar{\boldsymbol{p}},x_{\mathrm{L}}} (y^d - x_{\mathrm{L}}) \le \bar{G}^{\mathrm{M}}(T^d,\bar{\boldsymbol{p}},y^d) \tag{13}$$

and

$$\bar{G}^{\mathrm{M}}(T^d,\boldsymbol{p},x_{\mathrm{U}}) + \frac{\partial\bar{G}^{\mathrm{M}}}{\partial x}\Big|_{T^d,\bar{\boldsymbol{p}},x_{\mathrm{U}}} (y^d - x_{\mathrm{U}}) \le \bar{G}^{\mathrm{M}}(T^d,\bar{\boldsymbol{p}},y^d). \tag{14}$$

Similarly, we can check if parameter values $\bar{\boldsymbol{p}}$ fulfill conditions (11) and (12) by solving the subproblems

$$f^{(15)} = \max_{T\in\mathcal{T},y\in\mathcal{X}} \quad \bar{G}^{\mathrm{M}}(T,\bar{\boldsymbol{p}},x_{\mathrm{L}}) + \frac{\partial\bar{G}^{\mathrm{M}}}{\partial x}\Big|_{T,\bar{\boldsymbol{p}},x_{\mathrm{L}}} (y - x_{\mathrm{L}}) - \bar{G}^{\mathrm{M}}(T,\bar{\boldsymbol{p}},y) \tag{15}$$

and

$$f^{(16)} = \max_{T\in\mathcal{T},y\in\mathcal{X}} \quad \bar{G}^{\mathrm{M}}(T,\bar{\boldsymbol{p}},x_{\mathrm{U}}) + \frac{\partial\bar{G}^{\mathrm{M}}}{\partial x}\Big|_{T,\bar{\boldsymbol{p}},x_{\mathrm{U}}} (y - x_{\mathrm{U}}) - \bar{G}^{\mathrm{M}}(T,\bar{\boldsymbol{p}},y). \tag{16}$$

Again, if (the final lower bound of) the optimal objective value of (15) and (16) is less equal to $\varepsilon^{\mathrm{a},(15)}$ and $\varepsilon^{\mathrm{a},(16)}$, $\bar{\boldsymbol{p}}$ fulfills the corresponding conditions.

Secant strictly below $\bar{G}^{\mathrm{M}}$ in the interior of the phase split

In order to exclude additional phases from the predicted phase split, Mitsos et al. (2009a) additionally require that the secant, which is constructed approximately at the phase split, lies in the interior of the predicted phase split strictly below the Gibbs surface (case C in Mitsos et al., 2009a), c.f. Fig. 1d. As strict inequalities and open sets are difficult to handle numerically, a back-off $\delta_x > 0$ is introduced and the strict inequality is relaxed to

$$\bar{G}^{\mathrm{M}}(T,\bar{\boldsymbol{p}},x_1+\delta_x) + \frac{\bar{G}^{\mathrm{M}}(T,\bar{\boldsymbol{p}},x_2-\delta_x) - \bar{G}^{\mathrm{M}}(T,\bar{\boldsymbol{p}},x_1+\delta_x)}{(x_2-\delta_x)-(x_1+\delta_x)}\big(y-(x_1+\delta_x)\big) \le \bar{G}^{\mathrm{M}}(T,\boldsymbol{p},y),\ \forall T\in\mathcal{T},\ \forall y\in[x_1+\delta_x,x_2-\delta_x]. \tag{17}$$

Similar to (6), $\boldsymbol{x}$ depends on the temperature T and parameter values $\bar{\boldsymbol{p}}$. Reformulation, relaxation, and subsequent discretization, akin (6), yields

$$-\bar{G}^{\mathrm{M}}(T^d,\bar{\boldsymbol{p}},y^d) + \bar{G}^{\mathrm{M}}(T^d,\bar{\boldsymbol{p}},x_1^d+\delta_x) + \frac{\bar{G}^{\mathrm{M}}(T^d,\bar{\boldsymbol{p}},x_2^d-\delta_x) - \bar{G}^{\mathrm{M}}(T^d,\bar{\boldsymbol{p}},x_1^d+\delta_x)}{(x_2^d-\delta_x)-(x_1^d+\delta_x)}\big(y^d-(x_1^d+\delta_x)\big) \le 0. \tag{18}$$

Feasibility of parameter values $\bar{\boldsymbol{p}}$ in (17) can be checked by solving the subproblem

$$f^{(19)} = \max_{\substack{T\in\mathcal{T},y\in\mathcal{X},\\ \boldsymbol{x}\in\mathcal{X}^2}} \quad -\bar{G}^{\mathrm{M}}(T,\bar{\boldsymbol{p}},y+\delta_x) + \bar{G}^{\mathrm{M}}(T,\bar{\boldsymbol{p}},x_1+\delta_x) + \frac{\bar{G}^{\mathrm{M}}(T,\bar{\boldsymbol{p}},x_2-\delta_x) - \bar{G}^{\mathrm{M}}(T,\bar{\boldsymbol{p}},x_1+\delta_x)}{(x_2-\delta_x)-(x_1+\delta_x)}\big(y-(x_1+\delta_x)\big)$$
$$\text{s.t.} \quad x_1+\delta_x \le y \quad y \le x_2-\delta_x \quad (2) \text{ holds for } T,\bar{\boldsymbol{p}},\boldsymbol{x} \quad \text{mass balances hold for } \boldsymbol{x}, \tag{19}$$

which itself is an SIP with (4) being its corresponding LLP. If (the final lower bound of) the optimal objective value $f^{(19)}$ is less equal to a small $\varepsilon^{\mathrm{a},(19)}$, $\bar{\boldsymbol{p}}$ fulfills the corresponding condition. Otherwise the optimal solution T^* and y^* of (19) are used to discretize (18).

2.2. Optimal experimental design for guaranteed parameter estimation and its application to liquid-liquid equilibrium systems

The OED for GPE problem reads (Walz et al., 2018; Mukkula and Paulen, 2016a,b, 2017a)

$$\min_{T\in\mathcal{T}} \max_{\boldsymbol{p}_{j,i}\in\mathcal{P}(T)} \quad \sum_{i=1}^{n_{\mathrm{p}}} (p_{\mathrm{U},i,i} - p_{\mathrm{L},i,i})$$
$$\text{with } \mathcal{P}(T) = \left\{ \boldsymbol{p}\in\tilde{\mathcal{P}} \;\middle|\; \begin{array}{l} 2\eta_{\mathrm{L}} \le \hat{\boldsymbol{x}} - \boldsymbol{x} \\ 2\eta_{\mathrm{U}} \ge \hat{\boldsymbol{x}} - \boldsymbol{x} \\ \hat{\boldsymbol{x}} \text{ is the model system output for } T \text{ and } \hat{\boldsymbol{p}} \\ \boldsymbol{x} \text{ is the model system output for } T \text{ and } \boldsymbol{p} \end{array} \right\}, \tag{20}$$

where $\boldsymbol{p}_{j,i} = \left(p_{j,i,1},\dots,p_{j,i,n_{\mathrm{p}}}\right)^T$ with $j\in\mathcal{J}=\{\mathrm{L},\mathrm{U}\}$ and $i\in\mathcal{I}=\{1,\dots,n_{\mathrm{p}}\}$, $\tilde{\mathcal{P}}$ and $\mathcal{T}$ are subsets of the real numbers of dimension n_{p} and n_{T}, $\hat{\boldsymbol{p}}$ are the nominal parameter values, η_{L} and η_{U} denote the maximum upper- and lower measurement errors, and $\boldsymbol{x}$ is the measured model system output. In (20), we aim to find the experimental conditions $\boldsymbol{T}$ that minimize the size of the estimated feasible parameter set. Considering the trade-off between computational burden and precision, we pragmatically choose to over-approximate the size of the feasible parameter set using an orthotope, c.f., Fig. 2a, and minimize its circumference. This orthotope, which encloses the feasible parameter set, is defined by $2n_{\mathrm{p}}$ points in the parametric space, i.e., $\boldsymbol{p}_{\mathrm{L},i}$ and $\boldsymbol{p}_{\mathrm{U},i}$, each being a vector of size n_{p}. Extending the approach to other (tighter) convex over-approximations is straightforward, e.g., minimizing the volume of the orthotope, similar to A-optimal designs of statistical approaches that minimize the dimensions of the enclosing box around the joint confidence interval (Asprey and Macchietto, 2002). The nominal parameter values $\hat{\boldsymbol{p}}$ are known *a priori* and are consistent with the measurements, i.e., they are contained in $\mathcal{P}(\boldsymbol{T})$ (for all possible $\boldsymbol{T}$). Therefore, in OED for GPE, the feasible set of the lower level $\mathcal{P}(\boldsymbol{T})$ is never empty; in contrast to GPE, where this might be the case (Walz et al., 2018). Therefore, we call (20) a min-max BLP, analogous to BLPs where the lower level is also never infeasible. To obtain meaningful results, the number of experiments should be equal

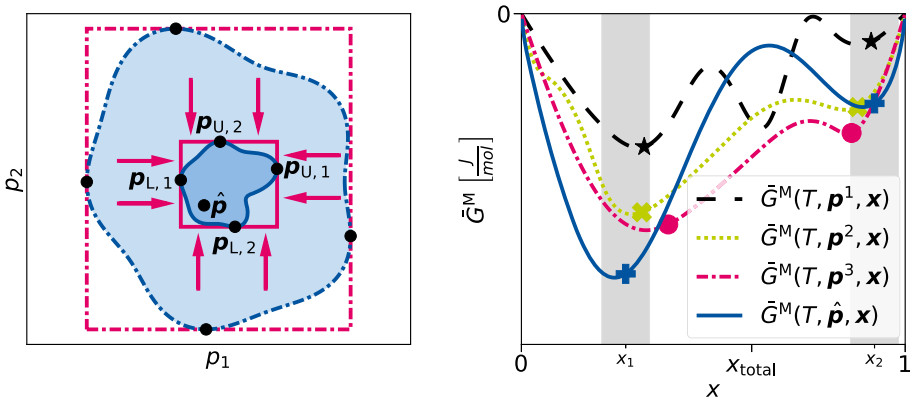

(a) (b)

Fig. 2. Visualization of the feasible parameter set, model outputs, and measurement uncertainty.
(a) Visualization of the feasible parameter set for $n_p = 2$ and aspired minimization of (the overapproximation) thereof. Based on Walz et al. (2018), Mukkula and Paulen (2016a).
(b) Visualization of the measurement uncertainty (shaded gray of width $\eta_U - \eta_L$) and $\bar{G}^M$ for different parameter values. The predicted phase split with the nominal parameter values $\hat{p}$ is denoted with x_1 and x_2, and parameters with superscripts denote different parameter values, i.e., $p^i \in \tilde{\mathcal{P}}$.

to the number of uncertain parameter values, i.e., $n_T = n_p$. Similar to Mukkula and Paulen (2017a), we assume that $\mathcal{P}$ is not limited by $\tilde{\mathcal{P}}$, i.e., $\partial\mathcal{P}(\boldsymbol{T}) \cap \tilde{\mathcal{P}} = \emptyset,\ \forall \boldsymbol{T}$. One could naively set $\tilde{\mathcal{P}} = \mathbb{R}^{n_P}$; however, this leads to profound implications for the employed solution algorithm, as discussed by Jungen et al. (2022) for the case of SIPs. Therefore, we pragmatically chose $\tilde{\mathcal{P}}$ as a compact set that is sufficiently large, c.f. Section 3.

For now, assume an analytical input-output relationship for $\boldsymbol{x}$ exists, i.e., we have an analytical function that gives us $\boldsymbol{x} = \boldsymbol{g}(\boldsymbol{T}, \boldsymbol{p})$. Fig. 2b shows, assuming such an analytical input-output relationship for the mole fractions $\boldsymbol{x}$ exists, the prediction of the LLE for different parameter values. The prediction with parameter values $\boldsymbol{p}^3$ is not within the measurement error, therefore not considered feasible.

In the following, we extend the OED for GPE approach to the case where the model output itself is implicitly defined by an optimization problem, as in the case for computing LLEs with (4). Hence, in contrast to previous works (Walz et al., 2018; Mukkula and Paulen, 2016a,b, 2017a), we are able to consider a vaster variety of systems. As a result, our solution procedure is adapted to the inclusion of additional (G)SIP constraints. Note that the applied solution strategy (to follow) requires that the solution of this optimization problem is unique. In our considered OED application, for a fixed total composition, we aim to find the optimal temperature to reduce the parameter uncertainty in the underlying excess model. We retain the introduced symbols from (20), and denote the scalar experimental design variable (optimal temperature) with $T \in \mathcal{T}$, andthe uncertain parameters of the underlying excess model with $\boldsymbol{p} \in \mathcal{P}$. We consider the mole fractions of the phases as the model outputs. Since, at a given temperature, the mole fractions of the phases are uniquely determined, the uniqueness assumption is fulfilled in our application. This is presumably the case in *real-world* as well as for our *predictions*. Note that extending to multiple experiments is conceptually straightforward but is omitted for notational convenience.

The resulting OED problem with rigorous LLE computations embedded reads

$$\min_{T\in\mathcal{T}} \max_{p_{j,i}\in\mathcal{P}(T)} \quad \sum_{i=1}^{n_p} \left(p_{U,i,i} - p_{L,i,i}\right)$$

$$\text{with} \quad \mathcal{P}(T) = \left\{ p \in \tilde{\mathcal{P}} \;\middle|\; \begin{array}{l} 2\eta_L \le \hat{x} - x \\ 2\eta_U \ge \hat{x} - x \\ (1) \text{ \& mass balances hold for } T, \hat{p}, \hat{x} \\ (1) \text{ \& mass balances hold for } T, p, x \\ (2) \text{ holds for } T, \hat{p}, \hat{x} \\ (2) \text{ holds for } T, p, x \\ (6) \text{ holds for } p \\ (11) \text{ holds for } p \\ (12) \text{ holds for } p \\ (17) \text{ holds for } p \end{array} \right\}. \tag{21}$$

We assume that the nominal parameter values $\hat{\boldsymbol{p}}$ fulfill the conditions (6), (11), (12), and (17). This is not restrictive as, e.g., the open-source software libDIPS (Jungen et al., 2023) comes with the capabilities of estimating parameter values, enforcing conditions like (6), (11), (12), and (17) on a temperature range.

Note that (21) is, by assumption, feasible. In contrast to previous work, the measured model system output is determined implicitly by (1), mass balances, and a semi-infinite constraint, i.e., (2). Additional semi-infinite and generalized semi-infinite constraints are imposed, i.e., the conditions of Mitsos et al. (2009a), to exclude *problematic* parameter values. Revisiting Fig. 2b, in addition to parameter values $\boldsymbol{p}^3$ (prediction not within measurement errors), now $\boldsymbol{p}^1$ and $\boldsymbol{p}^2$ are also not considered feasible. The prediction with $\boldsymbol{p}^1$ does not fulfill (17), and $\boldsymbol{p}^2$ does not fulfill (6).

Using the epigraph reformulation, we reformulate (21), eliminating the T–dependency of $\mathcal{P}(T)$, to

$$
\begin{aligned}
\min_{\substack{T\in\mathcal{T},\mu\in\mathbb{R},\\ \hat{\boldsymbol{x}},\boldsymbol{x}_{j,i}\in\mathcal{X}^2}} \quad & \mu \\
\text{s.t.} \quad & \left.\begin{array}{l} \sum_{i=1}^{n_\mathrm{p}} \left(p_{\mathrm{U},i,i} - p_{\mathrm{L},i,i}\right) - \mu \le 0 \\ \vee\, \exists j,i : \left\{\begin{array}{l} 2\eta_\mathrm{L} \le \hat{\boldsymbol{x}} - \boldsymbol{x}_{j,i} \vee \\ 2\eta_\mathrm{U} \ge \hat{\boldsymbol{x}} - \boldsymbol{x}_{j,i} \end{array}\right\} \end{array}\right\}, \ \forall p_{j,i} \in \mathcal{P} \\
& (1) \ \& \ \text{mass balances hold for } T, \hat{\boldsymbol{p}}, \hat{\boldsymbol{x}} \\
& (1) \ \& \ \text{mass balances hold for } T, \boldsymbol{p}, \boldsymbol{x}_{j,i} \\
& (2) \text{ holds for } T, \hat{\boldsymbol{p}}, \hat{\boldsymbol{x}} \\
& (2) \text{ holds for } T, \boldsymbol{p}, \boldsymbol{x}_{j,i},
\end{aligned}
\tag{22}
$$

$$
\text{with} \quad \mathcal{P} = \left\{ \boldsymbol{p} \in \tilde{\mathcal{P}} \;\middle|\; \begin{array}{l} (6) \text{ holds for } \boldsymbol{p} \\ (11) \text{ holds for } \boldsymbol{p} \\ (12) \text{ holds for } \boldsymbol{p} \\ (17) \text{ holds for } \boldsymbol{p} \end{array} \right\}.
$$

Note that we have introduced the additional variables μ, $\hat{\boldsymbol{x}}$, and $\boldsymbol{x}_{j,i}$, with $j \in \mathcal{J} = \{\mathrm{L}, \mathrm{U}\}$ and $i \in \mathcal{I} = \{1, \dots, n_\mathrm{p}\}$.

Discretizing (22) and relaxing the strict inequalities (akin Walz et al., 2018) yields the upper-level program

$$
\begin{aligned}
\min_{\substack{T\in\mathcal{T},\mu\in\mathbb{R},\\ \hat{\boldsymbol{x}},\boldsymbol{x}^d_{j,i}\in\mathcal{X}^2}} \quad & \mu \\
\text{s.t.} \quad & \left.\begin{array}{l} \sum_{i=1}^{n_\mathrm{p}} \left(p^d_{\mathrm{U},i,i} - p^d_{\mathrm{L},i,i}\right) - \mu \le 0 \\ \vee\, \exists j,i : \left\{\begin{array}{l} 2\eta_\mathrm{L} \ge \hat{\boldsymbol{x}} - \boldsymbol{x}^d_{j,i} \vee \\ 2\eta_\mathrm{U} \le \hat{\boldsymbol{x}} - \boldsymbol{x}^d_{j,i} \end{array}\right\} \end{array}\right\}, \qquad \forall d \in \mathcal{D}^{(23)} \\
& (1) \ \& \ \text{mass balances hold for } T, \hat{\boldsymbol{p}}, \hat{\boldsymbol{x}} \\
& (1) \ \& \ \text{mass balances hold for } T, \boldsymbol{p}, \boldsymbol{x}^d_{j,i}, \forall d \in \mathcal{D}^{(23)} \\
& (3) \text{ holds for } T, \hat{\boldsymbol{p}}, \hat{\boldsymbol{x}}, \qquad \forall l \in \mathcal{D}^{(3)} \\
& (3) \text{ holds for } T, \boldsymbol{p}^d_{j,i}, \boldsymbol{x}^d_{j,i}, \qquad \forall d \in \mathcal{D}^{(23)} \quad \forall l \in \mathcal{D}^{(3)}.
\end{aligned}
\tag{23}
$$

The conjunction in (23) can be reformulated using the min-operator, making it solvable with standard NLP solvers. Note that the number of optimization variables depends on the discretization $\mathcal{D}^{(23)}$. (23) has $4 + 2n_\mathrm{p}\left|\mathcal{D}^{(23)}\right|$ variables. (23) has (4) as an LLP for $\hat{\boldsymbol{x}}$ and for each $\boldsymbol{x}^d_{j,i}$. The solutions thereof are used to populate the set $\mathcal{D}^{(3)}$.

Although one discretization set $\mathcal{D}^{(3)}$ suffices, in the numerical case study in Section 3, a separate discretization set is introduced for each semi-infinite constraint. As a result, the number of constraints and, therefore, the computational burden is reduced.

To populate the discretization set $\mathcal{D}^{(23)}$, a medial-level problem, and in some cases an additional auxiliary problem (to follow) must be solved.

The medial-level problem is developed from

$$
\begin{aligned}
\max_{\substack{\boldsymbol{p}_{j,i}\in\tilde{\mathcal{P}},\\ \boldsymbol{x}_{j,i},\boldsymbol{x}^d_{c,j,i}\in\mathcal{X}}} \quad & \textstyle\sum_{i=1}^{n_\mathrm{p}} \left(p_{\mathrm{U},i,i} - p_{\mathrm{L},i,i}\right) - \bar{\mu} \\
\text{s.t.} \quad & 2\eta_\mathrm{L} \le \bar{\hat{\boldsymbol{x}}} - \boldsymbol{x}_{j,i} \\
& 2\eta_\mathrm{U} \ge \bar{\hat{\boldsymbol{x}}} - \boldsymbol{x}_{j,i} \\
& (1) \ \& \ \text{mass balances hold for } \bar{T}, \boldsymbol{p}, \boldsymbol{x}_{j,i} \\
& (2) \text{ holds for } \bar{T}, \boldsymbol{p}_{j,i}, \boldsymbol{x}_{j,i} \\
& (6) \text{ holds for } \boldsymbol{p}_{j,i} \\
& (11) \text{ holds for } \boldsymbol{p}_{j,i} \\
& (12) \text{ holds for } \boldsymbol{p}_{j,i} \\
& (17) \text{ holds for } \boldsymbol{p}_{j,i},
\end{aligned}
\tag{24}
$$

with $\bar{T}$, $\bar{\hat{\boldsymbol{x}}}$, and $\bar{\mu}$ being fixed to the optimal values of (23). Note that $\bar{\mu}$ is retained in the objective function solely for notational convenience. (24) computes the overapproximated feasible parameter set for a given temperature $\bar{T}$. Using the same strategy as before, discretizing yields

$$
\begin{aligned}
f^{(25)} = \max_{\substack{\boldsymbol{p}_{j,i}\in\tilde{\mathcal{P}},\\ \boldsymbol{x}_{j,i},\boldsymbol{x}^d_{c,j,i}\in\mathcal{X}}} \quad & \textstyle\sum_{i=1}^{n_\mathrm{p}} \left(p_{\mathrm{U},i,i} - p_{\mathrm{L},i,i}\right) - \bar{\mu} \\
\text{s.t.} \quad & 2\eta_\mathrm{L} \le \bar{\hat{\boldsymbol{x}}} - \boldsymbol{x}_{j,i} \\
& 2\eta_\mathrm{U} \ge \bar{\hat{\boldsymbol{x}}} - \boldsymbol{x}_{j,i} \\
& (1) \ \& \ \text{mass balances hold for } \bar{T}, \boldsymbol{p}_{j,i}, \boldsymbol{x}_{j,i} \\
& (3) \text{ holds for } \bar{T}, \boldsymbol{p}_{j,i}, \boldsymbol{x}_{j,i}, \qquad \forall l \in \mathcal{D}^{(3)} \\
& (3) \text{ holds for } T^d_{(7)}, \boldsymbol{p}_{j,i}, \boldsymbol{x}^d_{(7),j,i}, \qquad \forall d \in \mathcal{D}^{(7)}, \quad \forall l \in \mathcal{D}^{(3)} \\
& (7) \text{ holds for } T^d_{(7)}, \boldsymbol{p}_{j,i}, \boldsymbol{x}^d_{(7),j,i}, \qquad \forall d \in \mathcal{D}^{(7)} \\
& (3) \text{ holds for } T^d_{(8)}, \boldsymbol{p}_{j,i}, \boldsymbol{x}^d_{(8),j,i}, \qquad \forall d \in \mathcal{D}^{(8)}, \quad \forall l \in \mathcal{D}^{(3)} \\
& (8) \text{ holds for } T^d_{(8)}, \boldsymbol{p}_{j,i}, \boldsymbol{x}^d_{(8),j,i}, \qquad \forall d \in \mathcal{D}^{(8)} \\
& (13) \text{ holds for } \boldsymbol{p}_{j,i}, \qquad \forall d \in \mathcal{D}^{(13)} \\
& (14) \text{ holds for } \boldsymbol{p}_{j,i}, \qquad \forall d \in \mathcal{D}^{(14)} \\
& (3) \text{ holds for } T^d_{(18)}, \boldsymbol{p}_{j,i}, \boldsymbol{x}^d_{(18),j,i}, \qquad \forall d \in \mathcal{D}^{(18)}, \quad \forall l \in \mathcal{D}^{(3)} \\
& (18) \text{ holds for } T^d_{(18)}, \boldsymbol{p}_{j,i}, \boldsymbol{x}^d_{(18),j,i}, \qquad \forall d \in \mathcal{D}^{(18)},
\end{aligned}
\tag{25}
$$

with $c \in \mathcal{C} = \{(7), (8), (18)\}$. (25) has $6n_\mathrm{p}(1 + \left|\mathcal{D}^{(7)}\right|)$ variables. (25) has the following LLPs: (4) for $\hat{\boldsymbol{x}}$, each $\boldsymbol{x}_{j,i}$, and each $\boldsymbol{x}^d_{c,j,i}$; (9); (10); (15); (16); and (19), which are used to populate the respective discretized sets. Similar to the solution approach by Mitsos and Tsoukalas (2015), an auxiliary problem has to be solved to generate the discretization for $\mathcal{D}^{(23)}$ if no GSIP-like Slater point is obtained in (25). If a GSIP-like Slater point is already obtained in (25), its solution is used to populate $\mathcal{D}^{(23)}$. Note that it is also possible to solve a subproblem, which directly maximizes the semi-infinite constraint of (23), instead of first solving (25) and then, if necessary, an additional auxiliary problem. This approach is pursued by Djelassi et al. (2019) but comes with the drawback that this subproblem is of increased size. Our computational results in Section 3 (to follow) indicate that the complexity of the subproblem is a limiting factor, suggesting that this approach may not be optimal for our application.

For fixed $\bar{T}$, $\bar{\hat{\boldsymbol{x}}}$, and $\bar{\mu}$ from (23) and $\alpha > 0$, the auxiliary problem is defined as

$$
\begin{aligned}
f^{(26)} = \max_{\substack{\zeta\in\mathbb{R},\boldsymbol{p}_{j,i}\in\widetilde{\mathcal{P}},\\ \boldsymbol{x}_{j,i},\boldsymbol{x}^d_{c,j,i}\in\mathcal{X}}} \ & \zeta \\
\text{s.t. } \textstyle\sum_{i=1}^{n_\mathrm{p}} \left(p_{\mathrm{U},i,i} - p_{\mathrm{L},i,i}\right) - \bar{\mu} \geq \alpha f^{(25)} & \\
\boldsymbol{2}\eta_\mathrm{L} - \left(\bar{\hat{\boldsymbol{x}}} - \boldsymbol{x}_{j,i}\right) \leq \boldsymbol{1}\zeta & \\
-\boldsymbol{2}\eta_\mathrm{U} + \left(\bar{\hat{\boldsymbol{x}}} - \boldsymbol{x}_{j,i}\right) \leq \boldsymbol{1}\zeta & \\
\text{(1) \& mass balances hold for } \bar{T}, \boldsymbol{p}_{j,i}, \boldsymbol{x}_{j,i} & \\
\text{(3) holds for } \bar{T}, \boldsymbol{p}_{j,i}, \boldsymbol{x}_{j,i}, & \quad \forall l \in \mathcal{D}^{(3)} \\
\text{(3) holds for } T^d_{(7)}, \boldsymbol{p}_{j,i}, \boldsymbol{x}^d_{(7),j,i}, & \quad \forall d \in \mathcal{D}^{(7)}, \quad \forall l \in \mathcal{D}^{(3)} \\
\text{(7) holds for } T^d_{(7)}, \boldsymbol{p}_{j,i}, \boldsymbol{x}^d_{(7),j,i}, & \quad \forall d \in \mathcal{D}^{(7)} \\
\text{(3) holds for } T^d_{(8)}, \boldsymbol{p}_{j,i}, \boldsymbol{x}^d_{(8),j,i}, & \quad \forall d \in \mathcal{D}^{(8)}, \quad \forall l \in \mathcal{D}^{(3)} \\
\text{(8) holds for } T^d_{(8)}, \boldsymbol{p}_{j,i}, \boldsymbol{x}^d_{(8),j,i}, & \quad \forall d \in \mathcal{D}^{(8)} \\
\text{(13) holds for } \boldsymbol{p}_{j,i}, & \quad \forall d \in \mathcal{D}^{(13)} \\
\text{(14) holds for } \boldsymbol{p}_{j,i}, & \quad \forall d \in \mathcal{D}^{(14)} \\
\text{(3) holds for } T^d_{(18)}, \boldsymbol{p}_{j,i}, \boldsymbol{x}^d_{(18),j,i}, & \quad \forall d \in \mathcal{D}^{(18)}, \quad \forall l \in \mathcal{D}^{(3)} \\
\text{(18) holds for } T^d_{(18)}, \boldsymbol{p}_{j,i}, \boldsymbol{x}^d_{(18),j,i}, & \quad \forall d \in \mathcal{D}^{(18)}.
\end{aligned}
\tag{26}
$$

(26) has $6n_\mathrm{p}\left(1 + \left|D^{(7)}\right|\right) + 1$ variables. The subproblems and discretization procedures of (26) are identical to the ones of (25).

Given the above-defined subproblems, we can solve (21) by an adaptation of the algorithms proposed by Mitsos and Tsoukalas (2015), Djelassi et al. (2019), Falk and Hoffman (1977). From Djelassi et al. (2019), we adapt the idea to handle equality constraints, from Mitsos and Tsoukalas (2015), we adapt the idea to solve an auxiliary problem to generate the discretization, and from Falk and Hoffman (1977), we adapt the idea to use the solution of (25) as the upper-bound. The latter is also done by Walz et al. (2018). Note that these successors (Mitsos and Tsoukalas, 2015; Djelassi et al., 2019) utilize an upper-bounding procedure to find a global solution that is (SIP-)feasible, c.f., Definition 2 in Appendix B. However, in our application, the necessary assumption for the upper-bounding procedures is not satisfied due to the reformulations we applied. As a result, we rely solely on the relaxation-based lower-bounding procedure. The simplified pseudocode of the algorithmic adaption is given by Algorithm 1, which uses Algorithm 2 and Algorithm 3, see Appendix B, as subprocedures. Note that in the loop starting in Line 10 of Algorithm 2, we check conditions (7), (8), and (18). Therefore, we loop over $c \in C = \{(7), (8), (18)\}$.

Algorithm 1 and Algorithm 2 have the potential for parallelization, as the stability checks (Line 3 and 9 in Algorithm 1 and Lines 4 and 11 in Algorithm 2) and checks to avoid *problematic* parameter values (Lines 16, 22, and 27 in Algorithm 2) can be computed in parallel. This parallelization might increase scalability.

As the proposed algorithms are adaptations of Mitsos and Tsoukalas (2015), Djelassi et al. (2019), Falk and Hoffman (1977), which have been proven to converge within finite time, we argue in the following that their convergence guarantees are transferable to our adaptation. The assumptions necessary by Falk and Hoffman (1977) and Mitsos and Tsoukalas (2015) are included in Djelassi et al. (2019) which assume; Assumption 1: compact host sets; Assumption 2: continuous functions; Assumption 3: approximate solution of subproblems; Assumption 4: the solution of the coupling equality constraints is unique and exists; Assumption 5: the infimum of GSIP is equal to the optimum of the relaxed problem; Assumption 6: existence of ε^f-optimal GSIP-Slater point. Assumptions 1, 2, and 6 hold for our case. Assumptions 3 and 5 are standard technical assumptions. Assumption 4 of Djelassi et al. (2019) warrants further discussion. (1) is an equality constraint which couples the upper and media level, while (2) is a selection constraint, ensuring that the solution of (1), i.e., the predicted phase split, is unique. There exists a discretization of $\mathcal{D}^{(3)}$, such that when using criterion (2) and (used and discretized) condition (3) predict the same unique phase split (within some tolerance). Through the algorithm, we ensure that such a discretization is found. Now, assume parameter values are chosen by the solver (when solving (25)) that do not fulfill a condition reviewed in Section 2.1. These parameter values are subsequently excluded by solving the corresponding subproblem and refining the respective discretization(s), c.f., Algorithm 2. Therefore, *problematic* parameter values, which might produce non-unique predictions, are excluded. Note that while our argument provides an outline of the convergence proof for our algorithmic adaptation, a formal proof is beyond the scope of this contribution and will be addressed in future work.

3. Case study

As an illustrative case study, we use a 5$^{\text{th}}$-order Redlich-Kister model as the underlying $\bar{G}^\mathrm{E}$ model. The presented case study serves as a proof-of-concept, demonstrating the feasibility of our method while also highlighting the computational cost of the solution. Table 2 and 3 provides an overview of the used values. Pragmatically, we only consider parameter p_4 to be uncertain. Therefore, only p_4 is the nominal parameter with $\hat{p}_4 = p_4$. Note that p_4 is chosen for demonstrational purposes and further improvements to the (MI)NLP subsolvers are needed for real life applications including more uncertain parameters. The respective initial bounds $p_{4,\mathrm{lb}}$ and $p_{4,\mathrm{ub}}$ are given in Table 3. The set $\widetilde{\mathcal{P}}$ defined through $p_{4,\mathrm{lb}}$ and $p_{4,\mathrm{ub}}$ is arguably sufficiently large. This can be seen in Fig. 3b where the feasible parameter set is not restricted by $p_{4,\mathrm{lb}}$ or $p_{4,\mathrm{ub}}$. Recall that nominal parameters are known *a priori* and are assumed to be consistent with the measurements and model. All other Redlich-Kister parameters are considered to have no uncertainty, are fixed, and are equal to the values in Table 2. We selected parameter p_4 along with its uncertainty range for demonstrational purposes to show that our approach effectively works to exclude *problematic* parameter values not fulfilling the conditions reviewed in Section 2.1.2. Fig. 3a exemplary shows $\bar{G}^\mathrm{M}$ for different parameter values of p_4 and temperatures. For $p_4 = -12\,\mathrm{kJ\,mol^{-1}}$, $\bar{G}^\mathrm{M}$ is nonconvex on the left side of the phase split, violating (6) (and additionally (11)). Therefore, these parameter values are *problematic* and not considered feasible in our setting.

The estimated parameter uncertainty of p_4 for an additional measurement at the respective temperature is depicted in Fig. 3b. For $p_4 < -4.67\,\mathrm{kJ\,mol^{-1}}$, at least one of the conditions reviewed in Section 2.1 is violated for at least one temperature within $\mathcal{T}$ and, therefore, these values are not considered feasible. Because the conditions reviewed in Section 2.1 (and not the measurement uncertainty, i.e., $\boldsymbol{2}\eta_\mathrm{L} \leq \hat{\boldsymbol{x}} - \boldsymbol{x} \leq \boldsymbol{2}\eta_\mathrm{U}$), is restrictive for $p_{4,\mathrm{lb}}$, the predicted $p_{4,\mathrm{lb}}$ does not depend on the temperature. On the other hand, the predicted $p_{4,\mathrm{ub}}$ depends on the temperature because for larger values of p_4 the measurement uncertainty is restrictive.

We implemented Algorithms 1 and 2 in our open-source software libDIPS – Discretization-Based Semi-Infinite and Bilevel Programming Solvers (Jungen et al., 2023). Out of the box, libDIPS provides solvers for the deterministic global solution of (G)SIPs, existence-constrained SIPs, min-max programs, and BLPs with upper- and lower-levels of (MI)NLP type. For the solution of these hierarchical programs, adaptive discretization-based schemes are implemented. The implementation of Algorithms 1 and 2 is strongly based on existing solvers implemented in libDIPS and can be seen as an adaptation. For example, Algorithm 3, see Appendix B, is already provided in libDIPS and used in Algorithm 2 as a sub procedure. In the implementation, Algorithms 1 and 2 have been extended to support planning multiple experiments at different temperatures. This extension is straightforward: the conditions must hold for all planned experiments n_T and the corresponding subproblems must be extended for each planned experimental condition. Note that planning

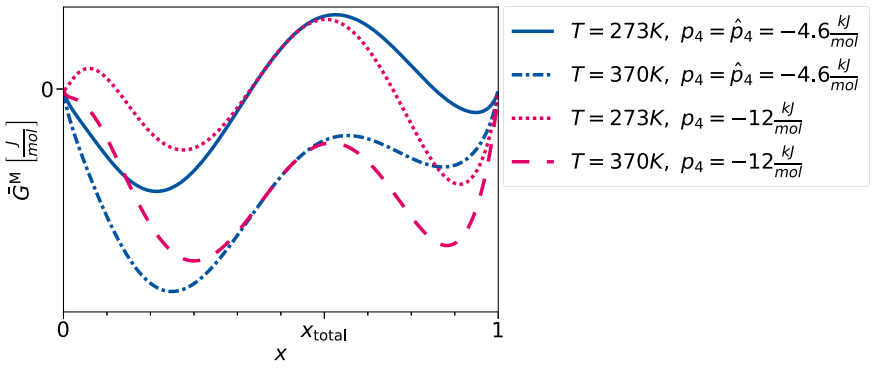

(a)

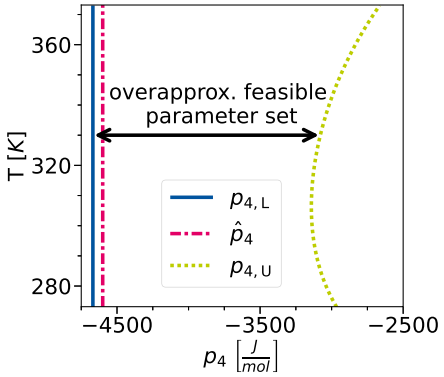

(b)

Fig. 3. Influence of p_4 on the curvature of $\bar{G}^M$ and estimated feasible parameter set. All other parameter values are set to the values given in, c.f., Table 2.
(a) $\bar{G}^M$ for different parameter values of p_4 and temperatures.
(b) Estimated parameter uncertainty of p_4 for an additional measurement at the respective temperature. Data generated by solving (25) for various temperature values within $\mathcal{T}$, in increments of one unit.

multiple experiments leads to more complex and an increased number of subproblems.

The computations are conducted on the RWTH High-Performance Computing cluster CLAIX running Rocky Linux 9 using on each core two Intel Xeon 8468 Sapphire processors running at 2.1 GHz with up to 2540 Mbit RAM and 96 cores per cluster node. All subproblems are solved using MAiNGO version 0.8.1 (Bongartz et al., 2018), configured to utilize CPLEX version 22.1.1 (IBM ILOG CPLEX v22, 2022) to solve (mixed-integer) linear programs and (mixed-integer) quadratic programs.

The optimal temperature for the next experiment is computed to be at 306 K with an estimated overapproximated feasible parameter set of $p_4 \in \left[-4.67\,\mathrm{kJ\,mol^{-1}}, -3.14\,\mathrm{kJ\,mol^{-1}}\right]$. This is in agreement with the brute-force prediction depicted in Fig. 3b. Considering the initial bounds on p_4, c.f., $\tilde{\mathcal{P}}$ in Table 3, the parameter uncertainty is reduced by 85 %. If the feasible parameter set is assumed to be already narrowed by the conditions reviewed in Section 2.1, the improvement is still 10 %. We would like to point out that even after performing OED for GPE, uncertainties (now reduced) remain in the parameter values, which in turn affect the model predictions.

Note that for the considered case study, condition (8) was never observed to be violated. However, it is still enforced for consistency reasons. We utilize one full cluster-node (96 cores) and terminate after 8 iterations (in Algorithm 1) and 11 min (wall-clock time). The overall computation is thus comparable to an LLE experiment, which often takes only 20 min to reach equilibrium (Pfennig, 2004). Recall, however, that the case study is only a proof-of-concept due to the simple thermodynamic model and the single uncertain parameter.

We also test whether the case study can be extended by incorporating additional uncertain parameters. For that purpose, additional to p_4 also p_5 is imposed with uncertainty, i.e, $p_{5,\mathrm{lb}} = 2.5\,\mathrm{kJ\,mol^{-1}}$, $p_{5,\mathrm{ub}} = 7.5\,\mathrm{kJ\,mol^{-1}}$, $\tilde{\mathcal{P}} = \left[p_{4,\mathrm{lb}}, p_{4,\mathrm{ub}}\right] \times \left[p_{5,\mathrm{lb}}, p_{5,\mathrm{ub}}\right]$. Recall that the number of planned experiments should be equal the number of uncertain parameters (Section 2.2). Hence, the corresponding subproblems are adapted for planning two experiments at (different) temperatures. As outlined in Section 3, the subproblems can be easily adapted for planning multiple experiments, and the implemented algorithms also support this. Note that considering two uncertain parameters would not be sufficient for real-world applications, where the number of uncertain parameters is usually much higher.

The resulting OED problem could not be solved by utilizing two full cluster-nodes (192 cores) and a maximum wall-clock time of 12 h. In the first iteration of Algorithm 1, the subproblems (23) and (4) are all solved in less than 30 s. Then, Algorithm 2 is called, and in the first main iteration, all subproblems and Algorithm 3, see Appendix B, used for checking and computing the discretization for (7), (8), and (18), terminate in less than 5 min. After discretization, (25) is intractable for MAiNGO[2]. After more than 11 h, the absolute gap is still 3.2×10^3. The upper and lower bounds reported by MAiNGO remain unchanged within this time, indicating that the optimal solution is most likely found during prepro-

[2] Since (25) can not be solved within a reasonable time, we are unable to compute the estimated parameter uncertainties at different temperatures, as was done in the brute-force prediction shown in Fig. 3b for the case of one uncertain parameter.

Algorithm 1: Simplified pseudocode for solving (21). All subproblems are solved globally. User inputs are the initial discretization sets $\mathcal{D}^{(23),0}$, $\mathcal{D}^{(3),0}$; parameters α_{init}, α_{red}; and tolerances ε^{a} (absolut optimality tolerance of the experimental design), $\varepsilon^{\text{a},(4)}$ (superscript and subscript numbers in parentheses indicate the corresponding equation). Outputs are the optimal objective value $f^{(23)}$ and optimal solution point $T^{(23)}$.

1 set $\mathcal{D}^{(23)} \leftarrow \mathcal{D}^{(23),0}$, $\mathcal{D}^{(3)} \leftarrow \mathcal{D}^{(3),0}$, $LBD \leftarrow -\infty$, and $UBD \leftarrow \infty$; `// initialize`
2 solve (23) to obtain $\mu^{(23)}$, $T^{(23)}$, $\hat{\boldsymbol{x}}^{(23)}$, and $\boldsymbol{x}_{j,i}^{d,(23)}$; `// compute exp. design`
`// check stability of` $\hat{\boldsymbol{x}}^{(23)}$ `using the TP critereon`
3 solve (4) for $T^{(23)}$, $\hat{\boldsymbol{p}}$, $\hat{\boldsymbol{x}}^{(23)}$ to obtain $f^{(4)}$ and $\boldsymbol{y}^*$;
4 **if** $f^{(4)} > \varepsilon^{\text{a},(4)}$ **then**
  `// TP critereon violated, refine discretization, & resolve (23)`
5 $\mathcal{D}^{(3)} \leftarrow \mathcal{D}^{(3)} \bigcup \{\boldsymbol{y}^*\}$;
6 go to Line 1;
7 **end**
`// check stability of` $\boldsymbol{x}_{j,i}^{d,(23)}$ `using the TP critereon`
8 **for** *all* $j, i, d \in \mathcal{J}, \mathcal{I}, \mathcal{D}^{(23)}$ **do**
9 solve (4) for $T^{(23)}$, $\boldsymbol{p}_{j,i}^{d}$, $\boldsymbol{x}_{j,i}^{d,(23)}$ to obtain $f^{(4)}$ and $\boldsymbol{y}^*$;
10 **if** $f^{(4)} > \varepsilon^{\text{a},(4)}$ **then**
   `// TP critereon violated, refine discretization, & resolve (23)`
11   $\mathcal{D}^{(3)} \leftarrow \mathcal{D}^{(3)} \bigcup \{\boldsymbol{y}^*\}$;
12   go to Line 1;
13 **end**
14 **end**
15 set $LBD \leftarrow \mu^{(23)}$; `// update lower bound`
`// check optimality of computed exp. design`
16 solve (25) using Algorithm 2 for fixed $T^{(23)}$ and $\mu^{(23)}$ to obtain $f^{(25)}$ and $\boldsymbol{p}_{j,i}^{(25)}$;
17 **if** $f^{(25)} > 0$ **then**
18 **if** $2\eta_{\text{L}} < \hat{\boldsymbol{x}}^{(23)} - \boldsymbol{x}_{j,i}^{(25)} \wedge 2\eta_{\text{U}} > \hat{\boldsymbol{x}}^{(23)} - \boldsymbol{x}_{j,i}^{(25)}$ **then**
   `// Slater condition fulfilled; refine discretization`
19   $\mathcal{D}^{(23)} \leftarrow \mathcal{D}^{(23)} \bigcup \boldsymbol{p}_{j,i}^{(25)}$
20 **else**
   `// generate valid discretization with (26) and refine discretization`
21   $\alpha \leftarrow \alpha_{\text{init}}$;
22   **do**
23   solve (26) using Algorithm 2 for fixed $T^{(23)}$, $\mu^{(23)}$, and $f^{(25)}$ to obtain $f^{(26)}$ and $\boldsymbol{p}_{j,i}^{(26)}$;
24    $\alpha \leftarrow \alpha / \alpha_{\text{red}}$;
25   **while** $f^{(26)} > 0$;
26   $\mathcal{D}^{(23)} \leftarrow \mathcal{D}^{(23)} \bigcup \boldsymbol{p}_{j,i}^{(26)}$
27 **end**
28 **else**
29 terminate; `// computed exp. design optimal`
30 **end**
31 **if** $f^{(25)} + \mu^{(23)} \leq UBD$ **then**
32 set $UBD \leftarrow f^{(25)} + \mu^{(23)}$; `// obtained better exp. design`
33 **end**
34 **if** $UBD - LBD < \varepsilon^{\text{a}}$ **then**
35 terminate; `// computed exp. design optimal`
36 **end**
37 Go to Line 1;

Algorithm 2: Simplified pseudocode for solving subproblem (SP), i.e., (25) or (26). All subproblems are solved globally. User inputs are the solution point of (23) $T^{(23)}$, $\mu^{(23)}$; the initial discretization sets $\mathcal{D}^{(3),0}$, $\mathcal{D}^{(7),0}$, $\mathcal{D}^{(8),0}$, $\mathcal{D}^{(13),0}$, $\mathcal{D}^{(18),0}$; parameters α_{init}, α_{red}; and tolerances $\varepsilon^{\text{a},(4)}$n, $\varepsilon^{\text{a},(7)}$, $\varepsilon^{\text{a},(8)}$, $\varepsilon^{\text{a},(18)}$, $\varepsilon^{\text{a},(15)}$, $\varepsilon^{\text{a},(16)}$ (superscript and subscript numbers in parentheses indicate the corresponding equation). Note that $c \in C = \{(7), (8), (18)\}$.

1 set $\mathcal{D}^{(3)} \leftarrow \mathcal{D}^{(3),0}$, $\mathcal{D}^{(7)} \leftarrow \mathcal{D}^{(7),0}$, $\mathcal{D}^{(8)} \leftarrow \mathcal{D}^{(8),0}$, $\mathcal{D}^{(13)} \leftarrow \mathcal{D}^{(13),0}$, $\mathcal{D}^{(18)} \leftarrow \mathcal{D}^{(18),0}$; `// initialize`
2 solve (SP) for fixed $T^{(23)}$ and $\mu^{(23)}$ to obtain $f^{(\text{SP})}$, $\boldsymbol{p}_{j,i}^{(\text{SP})}$, $\boldsymbol{x}_{j,i}^{(\text{SP})}$, and $\boldsymbol{x}_{c,j,i}^{d,(\text{SP})}$;
3 **for** *all* $j, i \in \mathcal{J}, \mathcal{I}$ **do**
  `// check stability of` $\boldsymbol{x}_{j,i}^{(\text{SP})}$ `using the TP critereon`
4 solve (4) for $T^{(23)}$, $\boldsymbol{p}_{j,i}^{(\text{SP})}$, $\boldsymbol{x}_{j,i}^{(\text{SP})}$ to obtain $f^{(4)}$ and $\boldsymbol{y}^*$;
5 **if** $f^{(4)} > \varepsilon^{\text{a},(4)}$ **then**
   `// TP critereon violated, refine discretization, & resolve (SP)`
6   $\mathcal{D}^{(3)} \leftarrow \mathcal{D}^{(3)} \bigcup \{\boldsymbol{y}^*\}$;
7   go to Line 2;
8 **end**
9 **end**
10 **for** *all* $c, j, i, d(c) \in \mathcal{J}, \mathcal{I}, C, D^c$ **do**
  `// check stability of` $x_{c,j,i}^{d,(\text{SP})}$ `using the TP critereon`
11 solve (4) for fixed T_c^d, $\boldsymbol{p}_{j,i}^{(\text{SP})}$, $\boldsymbol{x}_{c,j,i}^{d,(\text{SP})}$ to obtain $f^{(4)}$, and $\boldsymbol{y}^*$;
12 **if** $f^{(4)} > \varepsilon^{\text{a},(4)}$ **then**
   `// TP critereon violated, refine discretization, & resolve (SP)`
13   $\mathcal{D}^{(3)} \leftarrow \mathcal{D}^{(3)} \bigcup \{\boldsymbol{y}^*\}$;
14   go to Line 2;
15 **end**
  `// check condition` c `to avoid` *problematic* `parameter values`
16 solve (P-c) using Algorithm 3 for fixed $\boldsymbol{p}_{j,i}^{(\text{SP})}$ to obtain $f^{(\text{P-c})}$ and y^*;
17 **if** $f^{(\text{P-c})} > \varepsilon^{\text{a},(\text{c})}$ **then**
   `//` *problematic* `parameter values detected, refine discretization, & resolve (SP)`
18   $\mathcal{D}^{(c)} \leftarrow \mathcal{D}^{(c)} \bigcup \{y^*\}$;
19   go to Line 2;
20 **end**
21 **end**
`// check (15) to avoid` *problematic* `parameter values`
22 solve (15) for fixed $T^{(23)}$, $\boldsymbol{p}_{j,i}^{(\text{SP})}$ to obtain $f^{(15)}$, and y^*;
23 **if** $f^{(15)} > \varepsilon^{\text{a},(15)}$ **then**
  `//` *problematic* `parameter values detected, refine discretization, & resolve (SP)`
24 $\mathcal{D}^{(13)} \leftarrow \mathcal{D}^{(13)} \bigcup \{y^*\}$;
25 go to Line 2;
26 **end**
`// check (16) to avoid` *problematic* `parameter values`
27 solve (16) for fixed $T^{(23)}$, $\boldsymbol{p}_{j,i}^{(\text{SP})}$ to obtain $f^{(16)}$, and y^*;
28 **if** $f^{(16)} > \varepsilon^{\text{a},(16)}$ **then**
  `//` *problematic* `parameter values detected, refine discretization, & resolve (SP)`
29 $\mathcal{D}^{(14)} \leftarrow \mathcal{D}^{(14)} \bigcup \{y^*\}$;
30 go to Line 2;
31 **end**
32 return $f^{(\text{SP})}$ and $\boldsymbol{p}_{j,i}^{(\text{SP})}$;

Table 2
Redlich-Kister parameters used in the case study. Note that we only consider p_4 to be uncertain, i.e., only p_4 is a nominal parameter with $\hat{p}_4 = p_4$. All other parameters are considered to have no uncertainty.

Parameter	Value
p_1	$7\,\mathrm{kJ\,mol^{-1}}$
p_2	$4.5\,\mathrm{kJ\,mol^{-1}}$
p_3	$-4.5\,\mathrm{kJ\,mol^{-1}}$
p_4	$-4.6\,\mathrm{kJ\,mol^{-1}}$
p_5	$5\,\mathrm{kJ\,mol^{-1}}$

Table 3
Total composition, measurement bounds, temperature range, and initial parameter bounds used to define $\tilde{\mathcal{P}}$ in (21).

Parameter	Value
x_{total}	0.6
η_{L}	−0.01
η_{U}	0.01
$\mathcal{T}$	[273.15 K, 373.15 K]
$p_{4,\mathrm{lb}}$	$-12\,\mathrm{kJ\,mol^{-1}}$
$p_{4,\mathrm{ub}}$	$-2\,\mathrm{kJ\,mol^{-1}}$
$\tilde{\mathcal{P}}$	$[p_{4,\mathrm{lb}}, p_{4,\mathrm{ub}}]$

cessing. This motivates ad-hoc approaches which will be discussed in the next section.

4. Limitations and outlook

The overarching challenge of the OED for GPE approaches is that it comes with high computational costs. This is especially the case for our application because the embedded LLE computations and additional requirements to avoid *problematic* parameter values further increase the computational burden. We found that extending our approach to two uncertain parameters already becomes computationally infeasible, i.e., the employed subsolver does not solve the respective subproblems in a reasonable time. Due to this limitation, we can not answer the questions how our approach scales with multiple uncertain parameters and the size of the parameter set $\tilde{\mathcal{P}}$. The case study presented in Section 3, which considers a single uncertain parameter value, serves only as a proof-of-concept, demonstrating that our method is feasible. For real-world applications, the computational burden must first be reduced in order for our method to be applicable.

Reduction of the computational burden

We see potential for reducing the computation burden on four distinct levels: in the formulation itself, through the implementation of ad-hoc or heuristic approaches, within the hierarchical algorithms, and the utilized subsolvers.

In the formulation itself, simple reformulations, e.g., using a big-M formulation for reformulating the encountered conjunctions in the subproblems, as done by Walz et al. (2018), might already reduce the computation burden.

Simple ad-hoc or heuristic solution approaches are also possible. However, they come at the cost of losing rigor in computation. For example, Walz et al. (2018) terminate each optimization subproblem once a predefined time limit is reached. Through pre-mature termination no guarantee of global optimality within the subproblems is given. Walz et al. (2018) justify their ad-hoc approach by the non-changing upper bound reported by the subsolver during solution. We saw the same behavior in our case study. A non-changing upper bound is an indicator that the optimal solution has already been found. Note that the global solution of the subproblems is required for the employed solution algorithm. Hence, this ad-hoc solution approach should be treated with caution. Using tailored heuristics to the system at hand also holds potential to reduce the computational burden. Olaya et al. (2008) demonstrated that for a ternary liquid mixture with closed miscibility gaps, additional empirical constraints on the parameter values can be derived. In our application, this would result in a smaller search space, potentially speeding up computations.

At the level of the hierarchical algorithms for solving GSIPs and SIPs, there surely is hidden potential for speeding up the computations. For example, we demonstrated in Jungen and Mitsos (2024) that a slight adaptation of an existing adaptive discretization-based algorithm resulted in significant speed-ups. Seidel (2020), Djelassi (2020), Zingler and Mitsos (2025) investigate how the sensitivity information of the lower-level objective function might lead to fewer iterations necessary to converge. Recall that the optimal solution of the lower level is used for populating the discretization. Further recall, that these discretization points, in essence, cut off infeasible points, thereby iteratively improving the approximation. Seidel (2020), Djelassi (2020), Zingler and Mitsos (2025) show that this can reduce the number of iterations necessary to converge. The reason is that by using additional sensitivity information of the lower-level objective function, a larger set of points is excluded with each discretization point. However, incorporating this sensitivity information comes with the additional cost that the subproblems might become harder to solve, hinting that his approach may not be ideal for our application, especially since the subproblems are already computationally very expensive.

Moreover, at the level of subsolvers, custom relaxations of functions have been shown to have a significant impact on the computation time (Tawarmalani and Sahinidis, 2004; Floudas and Gounaris, 2009). In particular for NRTL, we have shown in Najman et al. (2019) that custom relaxations can significantly reduce the computation time of global optimization in chemical process design. However, therein, we assume constant parameter values, implying that generalization would be necessary for our OED application. Fortunately, the recent developments and improvements of (MI)NLP solvers give hope that even with (possibly) not-so-optimal computationally efficient algorithms for hierarchical programs, applications to real-world problems will become more and more feasible. This positive outlook is at least supported by the increasing number of publications and real-world applications in which hierarchical programs have been solved over the last decade.

Extensions and future work

Once numerical challenges are overcome, a quantitative comparison to classical OED approaches should be carried out. Further, extensions to more phases should be investigated. Recall that we pragmatically considered a binary two-phase LLE with non-vanishing phases. In real-world applications, binary systems at a given temperature and pressure exhibit predominantly at most one LLE split. Therefore, our restriction to only two phases seems warranted. However, the question remains of how to handle LLEs where phases disappear, and/or the total number of phases is not known *a priori*. Mitsos and Barton (2007) present an approach where the number of phases must not be known *a priori* to compute the LLE. Adapting the approach of Mitsos and Barton (2007) appears promising for overcoming this challenge. Furthermore, the overall composition should be considered an experimental design variable. Upon the successful implementation of these extensions, integrating the OED for GPE approach into process simulation software should be considered.

Other future work might entail tighter approximations of the feasible parameter set, as the orthotropic approximation is very pessimistic (Pronzato and Walter, 1990). Walz et al. (2018) note that for one of their case studies, the computed design leads to the smallest over-approximated feasible parameter set; however, this does not correspond to the actual smallest possible feasible parameter set.

Furthermore, tailoring the OED for GPE to the intended application remains the ultimate goal, as done by Walz et al. (2020). A comparison to statistical approaches, e.g., Fleitmann et al. (2021, 2022), remains to

be seen. However, one must note that such a comparison is difficult, as the *best* OED approach is likely strongly case-dependent.

5. Conclusion

Existing approaches of optimal experimental design (OED) for guaranteed parameter estimation (GPE) were not applicable to systems whose input-output relation is implicitly defined through an equation system and additional semi-infinite constraints. Examples of such systems are systems with embedded liquid-liquid equilibria (LLEs) which are modelled using a rigorous method, i.e., the Baker's criterion. Embedded LLE computations further complicate matters as *problematic* parameter values may be encountered which lead to erroneous predictions. To be able to incorporate LLE computations into the OED for GPE formulation, we extended an existing formulation and solution procedure. Further, we enforced additional requirements to avoid *problematic* parameter values.

In our numerical case study, we presented a proof-of-concept using the Redlich-Kister model to plan an OED that significantly reduced the predicted parameter uncertainty.

One of the main challenges encountered in OED for GPE approaches is the high computational costs of solving the subproblems. This is especially the case in our application as we use a rigorous formulation for modelling the embedded LLE. Due to computational costs, our proposed method is currently not feasible for real-world applications that typically involve multiple uncertain parameters. We propose four approaches to reduce computational effort: modifying the subproblem formulation, implementing ad-hoc or heuristic methods within the hierarchical algorithms, and within the subsolvers used. Finally, we outline extensions and future work, *once* computational challenges have been overcome.

Acronyms

BLP	bilevel program
GPE	guaranteed parameter estimation
GSIP	generalized semi-infinite program
LLE	liquid-liquid equilibrium
LLP	lower-level problem
NLP/(MI)NLP	(mixed-integer) nonlinear program
OED	optimal experimental design
SIP	semi-infinite program
TP	tangent plane

CRediT authorship contribution statement

Daniel Jungen: Writing – original draft, Visualization, Validation, Software, Methodology, Investigation, Formal analysis, Conceptualization; **Jan-Frederic Laub:** Writing – review & editing, Validation, Software, Investigation; **Alexander Mitsos:** Writing – review & editing, Supervision, Resources, Funding acquisition, Conceptualization.

Data availability

https://git.rwth-aachen.de/avt-svt/public/libdips

Declaration of generative AI and AI-assisted technologies in the writing process

During the preparation of this work, the authors utilized Grammarly's writing assistant tool and GPT language models developed by OpenAI to enhance the readability and language of the manuscript by generating ideas for improving previously drafted text. After using this tool/service, the authors reviewed and edited the content as needed and take full responsibility for the content of the publication.

Declaration of competing interest

The authors declare that they have no known competing financial interests or personal relationships that could have appeared to influence the work reported in this paper.

Acknowledgements

Funded by the Deutsche Forschungsgemeinschaft (DFG, German Research Foundation) under Germany´s Excellence Strategy - Cluster of Excellence 2186 "The Fuel Science Center" - ID: 390919832. Computations were performed with computing resources granted by RWTH Aachen University. We sincerely thank Aron Zingler for his careful reading of the manuscript and his helpful suggestions, which led to substantial improvements. We thank the anonymous reviewers for their constructive comments and valuable suggestions, which resulted in substantial improvements.

Appendix A. Liquid-liquid equilibrium model

A.1. Reduction of the model complexity

With the following assumptions, we can eliminate all describing state variables except for the mole fraction of the first species in the first phase and the mole fraction of the first species in the second phase. We consider two species and two phases, and assume that all species are present in all phases and non-vanishing phases. Recall that an extension to multi-component and multi-phase systems is conceptually straightforward. For notational convenience, we arbitrarily enforce that $x_{1,1} \leq x_{2,1}$, with $x_{l,i}$ being mole fraction of the i^{th} species in phase l. This directly leads to $x_{2,1} - x_{1,1} \geq \epsilon_{\text{split}} > 0$. Using the closing condition and the definition of the phase ratios φ_j, we obtain

$$\begin{aligned} x_{l,2} &= 1 - x_{l,2}, \ \forall l \\ \varphi_1 &= \frac{x_{2,1} - x_{1,\text{total}}}{x_{2,1} - x_{1,1}} \\ \varphi_2 &= 1 - \varphi_1. \end{aligned} \tag{A.1}$$

Eliminating the second component and dropping the subscript for the components, we obtain the simplified mass balances

$$\begin{aligned} x_1 - x_{\text{total}} &\leq 0 \\ x_{\text{total}} - x_2 &\leq 0 \\ x_1 + \epsilon_{\text{split}} - x_2 &\leq 0. \end{aligned} \qquad \text{(mass balances)}$$

A.2. Thermodynamic relations

The molar Gibbs free energy of mixing reads

$$\bar{G}^{\text{M}}\left(T, \boldsymbol{p}, \boldsymbol{x}_l\right) = \bar{\text{R}} T \sum_{c=1}^{n_{\text{c}}} x_{l,c} \ln x_{l,c} + \bar{G}^{\text{E}} \tag{A.2}$$

and is comprised of an ideal and an excess contribution. The molar excess Gibbs energy $\bar{G}^{\text{E}}$ stems from an excess model, in our case, the Redlich and Kister model. The $n_{\text{p}}{}^{\text{th}}$-order Redlich-Kister model reads for two components (Redlich and Kister, 1948)

$$\bar{G}^{\text{E}}\left(T, \boldsymbol{p}, \boldsymbol{x}_l\right) = \bar{\text{R}} T x_{l,1} x_{l,2} \sum_{i=0}^{n_p} p_i \left(x_{l,1} - x_{l,2}\right)^i, \tag{A.3}$$

with n_p denoting the number of parameters.

Appendix B. Blankenship and Falk solution algorithm for SIPs

The general formulation of an semi-infinite program (SIP) is given by

$$\begin{aligned} \min_{\boldsymbol{x}\in\mathcal{X}} \quad & f(\boldsymbol{x}) \\ \text{s.t.} \quad & \boldsymbol{g}^{\mathrm{u}}(\boldsymbol{x},\boldsymbol{y}) \leq \boldsymbol{0},\ \forall\ \boldsymbol{y}\in\mathcal{Y}, \\ \text{with} \quad & \mathcal{X} := \left\{\boldsymbol{x}\in\left[\boldsymbol{x}^{\mathrm{lb}},\boldsymbol{x}^{\mathrm{ub}}\right] : \boldsymbol{v}^{\mathrm{iu}}(\boldsymbol{x}) \leq \boldsymbol{0},\ \boldsymbol{v}^{\mathrm{eu}}(\boldsymbol{x}) = \boldsymbol{0}\right\} \\ & \mathcal{Y} := \left\{\boldsymbol{y}\in\left[\boldsymbol{y}^{\mathrm{lb}},\boldsymbol{y}^{\mathrm{ub}}\right] : \boldsymbol{v}^{\mathrm{il}}(\boldsymbol{y}) \leq \boldsymbol{0},\ \boldsymbol{v}^{\mathrm{el}}(\boldsymbol{y}) = \boldsymbol{0}\right\}, \end{aligned} \tag{B.1}$$

the objective function $f : \mathbb{R}^{n_{\mathrm{x}}} \to \mathbb{R}$, the semi-infinite constraint function $\boldsymbol{g}^{\mathrm{u}} : \mathbb{R}^{n_{\mathrm{x}}} \times \mathbb{R}^{n_{\mathrm{y}}} \to \mathbb{R}^{n_{\mathrm{gu}}}$, non-coupling upper-level equality and inequality constraints $\boldsymbol{v}^{\mathrm{iu}} : \mathbb{R}^{n_{\mathrm{x}}} \to \mathbb{R}^{n_{\mathrm{viu}}}$ and $\boldsymbol{v}^{\mathrm{eu}} : \mathbb{R}^{n_{\mathrm{x}}} \to \mathbb{R}^{n_{\mathrm{veu}}}$, non-coupling lower-level equality and inequality constraints $\boldsymbol{v}^{\mathrm{il}} : \mathbb{R}^{n_{\mathrm{y}}} \to \mathbb{R}^{n_{\mathrm{vil}}}$ and $\boldsymbol{v}^{\mathrm{el}} : \mathbb{R}^{n_{\mathrm{y}}} \to \mathbb{R}^{n_{\mathrm{vel}}}$. In the definition of the host sets $\mathcal{X}$ and $\mathcal{Y}$ the superscripts "lb" and "ub" denote finite upper bounds and lower bounds of the upper- and lower-level variables, respectively.

Definition 1 (ε^{a}-SIP-feasible point)**.** A point $\bar{\boldsymbol{x}} \in \mathcal{X}$ is ε^{a}-SIP-feasible in (B.1) if

$$\boldsymbol{g}^{\mathrm{u}}(\bar{\boldsymbol{x}},\boldsymbol{y}) \leq \varepsilon^{\mathrm{a}} \cdot \boldsymbol{1},\ \forall\ \boldsymbol{y}\in\mathcal{Y},$$

with $\varepsilon^{\mathrm{a}} \geq 0$.

Definition 2 (SIP-feasible point)**.** A point $\bar{\boldsymbol{x}} \in \mathcal{X}$ is called SIP-feasible in (B.1) if it fulfills Definition 1 (Definition 1) with $\varepsilon^{\mathrm{a}} = 0$.

Definition 3 (SIP-Slater point)**.** A point $\boldsymbol{x}^{\mathrm{S}} \in \mathcal{X}$ is called an SIP-Slater point in (B.1) if

$$\boldsymbol{g}^{\mathrm{u}}\left(\boldsymbol{x}^{\mathrm{S}},\boldsymbol{y}\right) < \boldsymbol{0},\ \forall\ \boldsymbol{y}\in\mathcal{Y}.$$

Definition 4 (ε^{f}-optimal SIP-Slater point)**.** A point $\boldsymbol{x}^{\mathrm{S}} \in \mathcal{X}$ is called an ε^{f}-optimal SIP-Slater point in (B.1) if

$$f\left(\boldsymbol{x}^{\mathrm{S}}\right) \leq f^{*} + \varepsilon^{\mathrm{f}} \wedge \boldsymbol{g}^{\mathrm{u}}\left(\boldsymbol{x}^{\mathrm{S}},\boldsymbol{y}\right) \leq -\varepsilon^{\mathrm{S}} \cdot \boldsymbol{1},\ \forall\ \boldsymbol{y}\in\mathcal{Y},$$

with $\varepsilon^{\mathrm{f}}, \varepsilon^{\mathrm{S}} > 0$, c.f., Lemma 2.4 in Mitsos (2011).

To solve (B.1) with the algorithm proposed by Blankenship and Falk (1976), c.f., Algorithm 3 in Appendix B, (B.1) is decomposed into (B.2) and (B.3) which read

$$\begin{aligned} f^{(\mathrm{B.2})} = \min_{\boldsymbol{x}\in\mathcal{X}} \quad & f(\boldsymbol{x}) \\ \text{s.t.} \quad & \boldsymbol{g}^{\mathrm{u}}\left(\boldsymbol{x},\boldsymbol{y}^{d}\right) \leq \boldsymbol{0},\ \forall\ \boldsymbol{y}^{d}\in\mathcal{Y}^{\mathrm{DISC}}, \\ \text{with} \quad & \mathcal{X} := \left\{\boldsymbol{x}\in\left[\boldsymbol{x}^{\mathrm{lb}},\boldsymbol{x}^{\mathrm{ub}}\right] : \boldsymbol{v}^{\mathrm{iu}}(\boldsymbol{x}) \leq \boldsymbol{0},\ \boldsymbol{v}^{\mathrm{eu}}(\boldsymbol{x}) = \boldsymbol{0}\right\}, \end{aligned} \tag{B.2}$$

with $\mathcal{Y}^{\mathrm{DISC}} \subsetneq \mathcal{Y}$, and

$$\begin{aligned} g^{(\mathrm{B.3})} = \max_{\boldsymbol{y}\in\mathcal{Y}} \quad & \max_{j\in\{1\ldots n_{\mathrm{gu}}\}} g^{\mathrm{u}}_{j}(\bar{\boldsymbol{x}},\boldsymbol{y}), \\ \text{with} \quad & \mathcal{Y} := \left\{\boldsymbol{y}\in\left[\boldsymbol{y}^{\mathrm{lb}},\boldsymbol{y}^{\mathrm{ub}}\right] : \boldsymbol{v}^{\mathrm{il}}(\boldsymbol{y}) \leq \boldsymbol{0},\ \boldsymbol{v}^{\mathrm{el}}(\boldsymbol{y}) = \boldsymbol{0}\right\}, \end{aligned} \tag{B.3}$$

Note that Algorithm 3 is already provided in libDIPS (Jungen et al., 2023). Algorithm 3 and its adaptations can be used to solve design problems involving embedded thermodynamic equilibrium (applied in Karacasulu et al., 2020; possible in, e.g., Gümüş, 1997; Clark and Westerberg, 1990; Clark, 1990).

Algorithm 3: Simplified pseudocode of the Blankenship and Falk algorithm to solve (B.1). All subproblems are solved globally. User inputs are the initial discretization $\mathcal{Y}^{0} \subsetneq \mathcal{Y}$ and feasibility tolerance $\varepsilon^{\mathrm{a}} \geq 0$.

```
set Y^DISC ← Y^0; // initialize
solve (B.2) to obtain f^(B.2) and x^(B.2);
solve (B.3) to obtain g^(B.3) and y^(B.3);
if g^(B.3) > ε^a then
    // candidate point x^(B.2) not ε^a-SIP-feasible, refine
       discretization, & resolve (B.2)
    Y^DISC ← Y^DISC ⋃ {y^(B.3)};
    go to Line 2
end
return f^(B.2) and x^(B.2);
```

References

IBM ILOG CPLEX v22 , 2022. Technical Report. International Business Machines Corporation.

Abrams, D.S., Prausnitz, J.M., 1975. Statistical thermodynamics of liquid mixtures: a new expression for the excess Gibbs energy of partly or completely miscible systems. AlChE J. 21, 116–128. https://doi.org/10.1002/aic.690210115

Asprey, S.P., Macchietto, S., 2002. Designing robust optimal dynamic experiments. J. Process Control 12, 545–556. https://doi.org/10.1016/S0959-1524(01)00020-8

Asprion, N., Böttcher, R., Mairhofer, J., Yliruka, M., Höller, J., Schwientek, J., Vanaret, C., Bortz, M., 2020. Implementation and application of model-based design of experiments in a flowsheet simulator. J. Chem. Eng. Data 65, 1135–1145. https://doi.org/10.1021/acs.jced.9b00494

Aster, R.C., Thurber, C.H., 2013. Parameter Estimation and Inverse Problems. Waltham MA, Academic Press. 2 ed.

Atkinson, A.C., Donev, A.N., Tobias, R., 2007. Optimum Experimental Designs, with SAS. Vol. 34. Oxford University Press, Oxford.

Baker, L.E., Pierce, A.C., Luks, K.D., 1982. Gibbs energy analysis of phase equilibria. Soc. Petroleum Eng. J. 22, 731–742. https://doi.org/10.2118/9806-PA

Belforte, G., Bona, B., Cerone, V., 1988. Parameter estimation with set membership uncertainty: Nonlinear families of models, in: 8th IFAC/IFOORS Symposium on Identification and System Parameter Estimation. Vol. 21. https://doi.org/10.1016/S1474-6670(17)54760-6

Belforte, G., Bona, B., Cerone, V., 1990. Parameter estimation algorithms for a set-membership description of uncertainty. Automatica 26, 887–898. https://doi.org/10.1016/0005-1098(90)90005-3

Belforte, G., Bona, B., Frediani, S., 1984. Optimal sampling schedule with unknown but bounded measurement errors: families of linear models. In: Haddad, A.H., Polis, K.P. (Eds.), Proceedings of the 23rd IEEE Conference on Decision and Control, pp. 1554–1559. https://doi.org/10.1109/CDC.1984.272342

Belforte, G., Bona, B., Frediani, S., 1987. Optimal sampling schedule for parameter estimation of linear models with unknown but bounded measurement errors. IEEE Trans. Automat. Control 32, 179–182. https://doi.org/10.1109/TAC.1987.1104535

Belforte, G., Gay, P., 2000. Optimal worst case estimation for LPV-FIR models with bounded errors. Proceedings of the 39th IEEE Conference on Decision and Control 5, 4573–4577. https://doi.org/10.1109/CDC.2001.914636

Belforte, G., Gay, P., 2004. Optimal worst case estimation for LPV-FIR models with bounded errors. Syst. Control Lett. 53, 259–268. https://doi.org/10.1016/j.sysconle.2004.05.004

Belforte, G., Tay, T.T., 1993. Optimal input design for worst-case system identification in $l_1/l_2/l_\infty$ 20, 273–278. https://doi.org/10.1016/0167-6911(93)90003-O

Blankenship, J.W., Falk, J.E., 1976. Infinitely constrained optimization problems. J. Optim. Theory Appl. 19, 261–281. https://doi.org/10.1007/BF00934096

Bollas, G.M., Barton, P.I., Mitsos, A., 2009. Bilevel optimization formulation for parameter estimation in vapor-liquid(-liquid) phase equilibrium problems. Chem. Eng. Sci. 64, 1768–1783. https://doi.org/10.1016/j.ces.2009.01.003

Bongartz, D., Najman, J., Sass, S., Mitsos, A., 2018. MAiNGO - McCormick-based Algorithm for mixed-integer Nonlinear Global Optimization. http://www.avt.rwth-aachen.de/global/show_document.asp?id=aaaaaaaaabclahw.

Borchers, S., Findeisen, R., 2011. Design of experiments for guaranteed parameter estimation in membership setting. In: Proceedings of the 50th IEEE Conference on Decision and Control and European Control Conference, pp. 2602–2607. https://doi.org/10.1109/CDC.2011.6161062

Borchers, S., Raković, S.V., Findeisen, R., 2011. Set membership parameter estimation and design of experiments using homothety. IFAC Proceedings Volumes 44, 9035–9040. https://doi.org/10.3182/20110828-6-IT-1002.03555

Box, G.E., Hill, W.J., 1967. Discrimination among mechanistic models. Technometrics 9, 57–71. https://doi.org/10.1080/00401706.1967.10490441

Chapman, W.G., Gubbins, K.E., Jackson, G., Radosz, M., 1990. New reference equation of state for associating liquids. Industr. Eng. Chem. Res. 29, 1709–1721. https://doi.org/10.1021/ie00104a021

Chen, G., Song, Z., Qi, Z., Sundmacher, K., 2021. Neural recommender system for the activity coefficient prediction and unifac model extension of ionic liquid-solute systems. AlChE J. 67. https://doi.org/10.1002/aic.17171

Clark, P.A., 1990. Bilevel programming for steady-state chemical process design - ii. performance study for nondegenerate problems. Comput. Chem. Eng. 14, 99–109. https://doi.org/10.1016/0098-1354(90)87008-D

Clark, P.A., Westerberg, A.W., 1990. Bilevel programming for steady-state chemical process design - i. fundamentals and algorithms. Comput. Chem. Eng. 14, 87–97. https://doi.org/10.1016/0098-1354(90)87007-C

Dai, W., Cremaschi, S., Subramani, H.J., Gao, H., 2019. Estimation of data uncertainty in the absence of replicate experiments. Chem. Eng. Res. Des. 147, 187–199. https://doi.org/10.1016/j.cherd.2019.05.007

Dechambre, D., Wolff, L., Pauls, C., Bardow, A., 2014. Optimal experimental design for the characterization of liquid-liquid equilibria. Industr. Eng. Chem. Res. 53, 19620–19627. https://doi.org/10.1021/ie5035573

Dempe, S., 2002. Vol. 61 of *New York*. Kluwer Academic Publishers.
Denis-Vidal, L., Jauberthie, C., Kieffer, M., 2019. Optimal experiment design for bounded-error estimation of nonlinear models. In: Wit, C. C.D., Sepulchre, R. (Eds.), Proceedings of the 58th IEEE Conference on Decision and Control, pp. 4147–4154. https://doi.org/10.1109/CDC40024.2019.9030003
Djelassi, H., 2020. Discretization-Based Algorithms for the Global Solution of Hierarchical Programs. Dissertation. RWTH Aachen University. Aachen, Germany. https://doi.org/10.18154/RWTH-2020-09163
Djelassi, H., Glass, M., Mitsos, A., 2019. Discretization-based algorithms for generalized semi-infinite and bilevel programs with coupling equality constraints. J. Global Optim. 75, 341–392. https://doi.org/10.1007/s10898-019-00764-3
Djelassi, H., Mitsos, A., Stein, O., 2021. Recent advances in nonconvex semi-infinite programming: applications and algorithms. EURO J. Comput. Optimiz. 9, 100006. https://doi.org/10.1016/j.ejco.2021.100006
Dong, Q., Chirico, R.D., Yan, X., Hong, X., Frenkel, M., 2005. Uncertainty reporting for experimental thermodynamic properties. J. Chem. Eng. Data 50, 546–550. https://doi.org/10.1021/je049673d
Duarte, B.P., Atkinson, A.C., Granjo, J.F., Oliveira, N.M., 2019. Optimal design of experiments for liquid-liquid equilibria characterization via semidefinite programming. Processes 7, 834. https://doi.org/10.3390/pr7110834
DECHEMA e.V., 2024. DECHEMA Data Preparation Package (DPP). https://i-systems.dechema.de/MyDECHEMA/DPP-Tutorials.htm.
Eubank, P.T., Elhassan, A.E., Barrufet, M.A., Whiting, W.B., 1992. Area method for prediction of fluid-phase equilibria. Industr. Eng. Chem. Res. 31, 942–949. https://doi.org/10.1021/ie00003a041
Eubank, P.T., Hall, K.R., 1995. Equal area rule and algorithm for determining phase compositions. AlChE J. 41, 924–927. https://doi.org/10.1002/aic.690410419
Falk, J.E., Hoffman, K., 1977. A nonconvex max-min problem. Naval Res. Logist. Quart. 24, 441–450. https://doi.org/10.1002/nav.3800240307
Fleitmann, L., Pyschik, J., Wolff, L., Schilling, J., Bardow, A., 2022. Optimal experimental design of physical property measurements for optimal chemical process simulations. Fluid Phase Equilib. 557, 113420. https://doi.org/10.1016/j.fluid.2022.113420
Fleitmann, L., Pyschik, J., Wolff, L. W.M., Bardow, A., 2021. Optimal Physical Property Data For Process Simulations by Optimal Experimental Design. Vol. 50. Elsevier BV. https://doi.org/10.1016/B978-0-323-88506-5.50133-9
Floudas, C.A., Gounaris, C.E., 2009. A review of recent advances in global optimization. J. Global Optim. 45, 3–38. https://doi.org/10.1007/s10898-008-9332-8
Franceschini, G., Macchietto, S., 2008. Model-based design of experiments for parameter precision: state of the art. Chem. Eng. Sci. 63, 4846–4872. https://doi.org/10.1016/j.ces.2007.11.034
Glass, M., Aigner, M., Viell, J., Jupke, A., Mitsos, A., 2017. Liquid-liquid equilibrium of 2-methyltetrahydrofuran/water over wide temperature range: measurements and rigorous regression. Fluid Phase Equilib. 433, 212–225. https://doi.org/10.1016/j.fluid.2016.11.004
Glass, M., Djelassi, H., Mitsos, A., 2018. Parameter estimation for cubic equations of state models subject to sufficient criteria for thermodynamic stability. Chem. Eng. Sci. 192, 981–992. https://doi.org/10.1016/j.ces.2018.08.033
Glass, M., Mitsos, A., 2017. Thermodynamic analysis of formulations to discriminate multiple roots of cubic equations of state in process models. Comput. Chem. Eng. 106, 407–420. https://doi.org/10.1016/j.compchemeng.2017.06.023
Glass, M., Mitsos, A., 2019. Parameter estimation in reactive systems subject to sufficient criteria for thermodynamic stability. Chem. Eng. Sci. 197, 420–431. https://doi.org/10.1016/j.ces.2018.08.035
Gomis, A.M., 2011. G^E models and algorithms for condensed phase equilibrium data regression in ternary systems: limitations and proposals. The Open Thermodyn. J. 5, 48–62. https://doi.org/10.2174/1874396X01105010048
Gross, J., Sadowski, G., 2001. Perturbed-chain saft: an equation of state based on a perturbation theory for chain molecules. Industr. Eng. Chem. Res. 40, 1244–1260. https://doi.org/10.1021/ie0003887
Gross, J., Vrabec, J., 2006. An equation-of-state contribution for polar components: dipolar molecules. AlChE J. 52, 1194–1204. https://doi.org/10.1002/aic.10683
Gümüş, Z.H., 1997. Reactive distillation column design with vapor/liquid/liquid equilibria. Comput. Chem. Eng. 21, 983–988. https://doi.org/10.1016/S0098-1354(97)00177-4
Hasenauer, J., Waldherr, S., Wagner, K., Allgöwer, F., 2010. Parameter identification, experimental design and model falsification for biological network models using semidefinite programming. IET Syst. Biol. 4, 119–130. https://doi.org/10.1049/iet-syb.2009.0030
Jirasek, F., Bamler, R., Fellenz, S., Bortz, M., Kloft, M., Mandt, S., Hasse, H., 2022. Making thermodynamic models of mixtures predictive by machine learning: matrix completion of pair interactions. Chem. Sci. 13, 4854–4862. https://doi.org/10.1039/D1SC07210B
Jungen, D., Djelassi, H., Mitsos, A., 2022. Adaptive discretization-based algorithms for semi-infinite programs with unbounded variables. Mathem. Methods Oper. Res. 96, 83–112. https://doi.org/10.1007/s00186-022-00792-y
Jungen, D., Mitsos, A., 2024. An improved oracle adaption for bilevel programs. Vol. 53. Elsevier. https://doi.org/10.1016/B978-0-443-28824-1.50551-2
Jungen, D., Zingler, A., Djelassi, H., Mitsos, A., 2023. libDIPS - discretization-based semi-infinite and bilevel programming solvers. 2025/06/09. https://optimization-online.org/?p=24914.
Karacasulu, K., Jungen, D., Najman, J., Bongartz, D., Grave, L., Mitsos, A., 2020. Design with equilibrium processes embedded: global optimization with guaranteed phase stability. In: 2020 Virtual AIChE Annual Meeting.
Karimshoushtari, M., Novara, C., 2020. Design of experiments for nonlinear system identification: a set membership approach. Automatica 119, 109036. https://doi.org/10.1016/j.automatica.2020.109036
Klamt, A., 1995. Conductor-like screening model for real solvents: a new approach to the quantitative calculation of solvation phenomena. J. Phys. Chem. 99, 2224–2235. https://doi.org/10.1021/j100007a062
Kontogeorgis, G.M., Dohrn, R., Economou, I.G., Hemptinne, J.-C.D., Kate, A., Kuitunen, S., Mooijer, M., Žilnik, L.F., Vesovic, V., 2021. Industrial requirements for thermodynamic and transport properties: 2020. Industr. Eng. Chem. Res. 60, 4987–5013. https://doi.org/10.1021/acs.iecr.0c05356
Marcilla, A., Martínez-Rodríguez, M., Olaya, M. M.D., 2025. The reliability of published lle correlation parameters in phase equilibria: a continuing challenge. https://doi.org/10.1021/acs.jced.5c00107
Marcilla, A., Olaya, M.M., Serrano, M.D., Reyes-Labarta, J.A., 2010. Aspects to be considered for the development of a correlation algorithm for condensed phase equilibrium data of ternary systems. Industr. Eng. Chem. Res. 49, 10100–10110. https://doi.org/10.1021/ie1010383
Marcilla, A., Reyes-Labarta, J.A., Olaya, M.M., 2017. Should we trust all the published lle correlation parameters in phase equilibria? Necessity of their assessment prior to publication. Fluid Phase Equilib. 433, 243–252. https://doi.org/10.1016/j.fluid.2016.11.009
Marvel, S.W., Williams, C.M., 2012. Set membership experimental design for biological systems. BMC Syst. Biol. 6, 21. https://doi.org/10.1186/1752-0509-6-21
Medina, E. I.S., Linke, S., Stoll, M., Sundmacher, K., 2022. Graph neural networks for the prediction of infinite dilution activity coefficients. Digital Discov. 1, 216–225. https://doi.org/10.1039/D1DD00037C
Medina, E. I.S., Linke, S., Stoll, M., Sundmacher, K., 2023. Gibbs-Helmholtz graph neural network: capturing the temperature dependency of activity coefficients at infinite dilution. Digital Discov. 2, 781–798. https://doi.org/10.1039/D2DD00142J
Michelsen, M.L., 1982a. The isothermal flash problem. Part I. Stability. Fluid Phase Equilibria 9, 1–19. https://doi.org/10.1016/0378-3812(82)85001-2
Michelsen, M.L., 1982b. The isothermal flash problem. Part II. Phase-split calculation. Fluid Phase Equilib. 9, 21–40. https://doi.org/10.1016/0378-3812(82)85002-4
Milanese, M., Belforte, G., 1982. Estimation theory and uncertainty intervals evaluation in presence of unknown but bounded errors: linear families of models and estimators. IEEE Trans. Automat. Control 27, 408–414. https://doi.org/10.1109/TAC.1982.1102926
Milanese, M., Vicino, A., 1991. Optimal estimation theory for dynamic systems with set membership uncertainty. Automatica 27, 997–1009. https://doi.org/10.1016/0005-1098(91)90134-N
Mitsos, A., 2011. Global optimization of semi-infinite programs via restriction of the right-hand side. Optimization 60, 1291–1308. https://doi.org/10.1080/02331934.2010.527970
Mitsos, A., Barton, P.I., 2007. A dual extremum principle in thermodynamics. AlChE J. 53, 2131–2147. https://doi.org/10.1002/aic.11230
Mitsos, A., Bollas, G.M., Barton, P.I., 2009a. Bilevel optimization formulation for parameter estimation in liquid-liquid phase equilibrium problems. Chem. Eng. Sci. 64, 548–559. https://doi.org/10.1016/j.ces.2008.09.034
Mitsos, A., Bollas, G.M., Barton, P.I., 2009b. Model and parameter identification in phase equilibria. Vol. 26. Elsevier. https://doi.org/10.1016/S1570-7946(09)70100-2
Mitsos, A., Glass, M., Hoffmann, T., 2018. Bilevel optimization algorithm for rigorous & robust parameter estimation in thermodynamics: BOARPET. https://www.avt.rwth-aachen.de/cms/avt/forschung/sonstiges/software/kvkz/boarpet/.
Mitsos, A., Tsoukalas, A., 2015. Global optimization of generalized semi-infinite programs via restriction of the right hand side. J. Global Optim. 61, 1–17. https://doi.org/10.1007/s10898-014-0146-6
Mukkula, A. R.G., Mateáš, M., Fikar, M., Paulen, R., 2021. Robust multi-stage model-based design of optimal experiments for nonlinear estimation. Comput. Chem. Eng. 155, 107499. https://doi.org/10.1016/j.compchemeng.2021.107499
Mukkula, A. R.G., Paulen, R., 2016a. Optimal design of dynamic experiments for guaranteed parameter estimation. In: Abramovitch, D., Chiu, G. (Eds.), American Control Conference, pp. 1826–1831. https://doi.org/10.1109/ACC.2016.7525184
Mukkula, A. R.G., Paulen, R., 2016b. Optimal dynamic experiment design for guaranteed parameter estimation. Vol. 38. Elsevier BV. https://doi.org/10.1016/B978-0-444-63428-3.50131-4
Mukkula, A. R.G., Paulen, R., 2017a. Model-based design of optimal experiments for nonlinear systems in the context of guaranteed parameter estimation. Comput. Chem. Eng. 99, 198–213. https://doi.org/10.1016/j.compchemeng.2017.01.029
Mukkula, A. R.G., Paulen, R., 2017b. Robust model-based design of experiments for guaranteed parameter estimation. Vol. 40. Elsevier. https://doi.org/10.1016/B978-0-444-63965-3.50275-0
Mukkula, A. R.G., Paulen, R., 2022. Robust design of optimal experiments considering consecutive re-designs. IFAC-PapersOnLine 55, 13–18. https://doi.org/10.1016/j.ifacol.2022.07.415
Najman, J., Bongartz, D., Mitsos, A., 2019. Relaxations of thermodynamic property and costing models in process engineering. Comput. Chem. Eng. 130, 106571. https://doi.org/10.1016/j.compchemeng.2019.106571
Nhu, N.V., Singh, M., Leonhard, K., 2008. Quantum mechanically based estimation of perturbed-chain polar statistical associating fluid theory parameters for analyzing their physical significance and predicting properties. J. Phys. Chem. B 112, 5693–5701. https://doi.org/10.1021/jp7105742
Norton, J.P., 1987. Identification and application of bounded-parameter models. Automatica 23, 497–507. https://doi.org/10.1016/0005-1098(87)90079-3
Olaya, M.M., Reyes-Labarta, J.A., Velasco, R., Ibarra, I., Marcilla, A., 2008. Modelling liquid-liquid equilibria for island type ternary systems. Fluid Phase Equilib. 265, 184–191. https://doi.org/10.1016/j.fluid.2007.12.010
Pfennig, A., 2004. Thermodynamik der Gemische. Berlin and New York, Springer.
Pronzato, L., 2008. Optimal experimental design and some related control problems. Automatica 44, 303–325. https://doi.org/10.1016/j.automatica.2007.05.016

Pronzato, L., Walter, E., 1989. Experiment design in a bounded-error context: comparison with D-optimality. Automatica 25, 383–391. https://doi.org/10.1016/0005-1098(89)90006-X

Pronzato, L., Walter, E., 1990. Experiment design for bounded-error models. Math. Comput. Simul. 32, 571–584. https://doi.org/10.1016/0378-4754(90)90013-9

Qin, S., Jiang, S., Li, J., Balaprakash, P., Lehn, R. C.V., Zavala, V.M., 2023. Capturing molecular interactions in graph neural networks: a case study in multi-component phase equilibrium. Digital Discov. 2, 138–151. https://doi.org/10.1039/D2DD00045H

Redlich, O., Kister, A.T., 1948. Algebraic representation of thermodynamic properties and the classification of solutions. Industr. Eng. Chem. 40, 345–348. https://doi.org/10.1021/ie50458a036

Renon, H., Prausnitz, J.M., 1968. Local compositions in thermodynamic excess functions for liquid mixtures. AlChE J. 14, 135–144. https://doi.org/10.1002/aic.690140124

Sørensen, J. M.S., Magnussen, T., Rasmussen, P., Fredenslund, A., 1979. Liquid-liquid equilibrium data: their retrieval, correlation and prediction: Part II: correlation. Fluid Phase Equilib. 3, 47–82. https://doi.org/10.1016/0378-3812(79)80027-8

Reyes-Labarta, J.A., Olaya, M.M., Velasco, R., Serrano, M.D., Marcilla, A., 2009. Correlation of the liquid-liquid equilibrium data for specific ternary systems with one or two partially miscible binary subsystems. Fluid Phase Equilib. 278, 9–14. https://doi.org/10.1016/j.fluid.2008.12.002

Rittig, J.G., Hicham, K.B., Schweidtmann, A.M., Dahmen, M., Mitsos, A., 2023. Graph neural networks for temperature-dependent activity coefficient prediction of solutes in ionic liquids. Comput. Chem. Eng. 171, 108153. https://doi.org/10.1016/j.compchemeng.2023.108153

Rustem, B., Howe, M., 2002. Algorithms for Worst-Case Design and Applications to Risk Management. Princeton University Press, Princeton N. J. and Oxford.

Sapkowski, M., Hofman, T., 2023. Problems and limitations in the calculation of liquid-liquid equilibrium. Fluid Phase Equilib. 571, 113823. https://doi.org/10.1016/j.fluid.2023.113823

Schweppe, F.C., 1968. Recursive state estimation: unknown but bounded errors and system inputs. IEEE Trans. Automat. Control 13, 22–28. https://doi.org/10.1109/TAC.1968.1098790

Seidel, T., 2020. Solving Semi-infinite Optimization Problems with Quadratic Rate of Convergence. Dissertation. Fraunhofer-Institut für Techno- und Wirtschaftsmathematik ITWM. Kaiserslautern. https://doi.org/10.24406/publica-fhg-283154

Stephan, P., Schaber, K., Stephan, K., Mayinger, F., 2017. Thermodynamik: Mehrstoffsysteme und chemische Reaktionen. Vol. 2 of *Berlin Heidelberg*. Springer.

Tawarmalani, M., Sahinidis, N.V., 2004. Global optimization of mixed-integer nonlinear programs: a theoretical and computational study. Math. Program. 99, 563–591. https://doi.org/10.1007/s10107-003-0467-6

Tsuboka, T., Katayama, T., 1975. Modified wilson equation for vapor-liquid and liquid-liquid equilibria. J. Chem. Eng. Jpn. 8, 181–187. https://doi.org/10.1252/jcej.8.181

Žaković, S., Rustem, B., 2003. Semi-infinite programming and applications to minimax problems. Ann. Oper. Res. 124, 81–110. https://doi.org/10.1023/B:ANOR.0000004764.76984.30

Walter, E., Piet-Lahanier, H., 1990. Estimation parameter bounds from bounded-error data: a survey. Math. Comput. Simul. 32, 449–468. https://doi.org/10.1016/0378-4754(90)90002-Z

Walz, O., Djelassi, H., Caspari, A., Mitsos, A., 2018. Bounded-error optimal experimental design via global solution of constrained min-max program. Comput. Chem. Eng. 111, 92–101. https://doi.org/10.1016/j.compchemeng.2017.12.016

Walz, O., Djelassi, H., Mitsos, A., 2020. Optimal experimental design for optimal process design: a trilevel optimization formulation. AlChE J. 66, 307. https://doi.org/10.1002/aic.16788

Welsh, J.S., Rojas, C.R., 2009. A Scenario Based Approach to Robust Experiment Design. Vol. 42. Elsevier Science Direct - IFAC PapersOnline. https://doi.org/10.3182/20090706-3-FR-2004.00031

Winter, B., Winter, C., Schilling, J., Bardow, A., 2022. A smile is all you need: predicting limiting activity coefficients from smiles with natural language processing. Digital Discov. 1, 859–869. https://doi.org/10.1039/D2DD00058J

Zingler, A., Mitsos, A., 2025. Derivative-enhanced lower-bounding in adaptive discretization for the global solution of semi-infinite optimization problems. Optim., 1–34. https://doi.org/10.1080/02331934.2025.2571756